

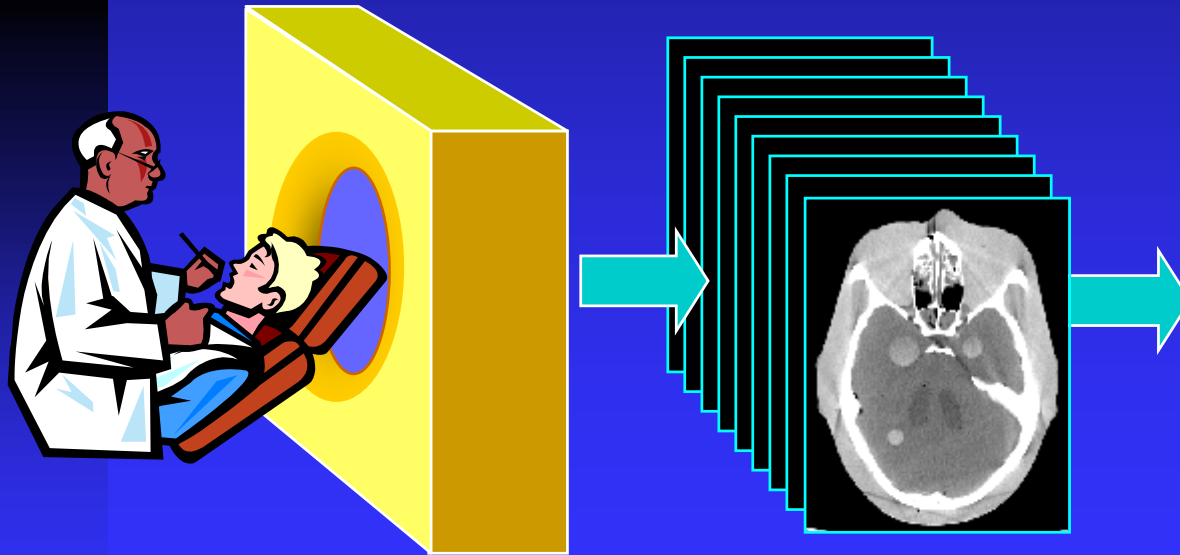
Multi-slice CT Image Reconstruction

Jiang Hsieh, Ph.D.

Applied Science Laboratory, GE Healthcare Technologies

Image Generation

- Reconstruction of images from projections.
 - ◆ “textbook” reconstruction
 - ◆ advanced acquisition (helical, cone beam)
 - ◆ advanced application (cardiac)
- Formulation of 2D images to 3D volume.



Reconstruction

Presentation



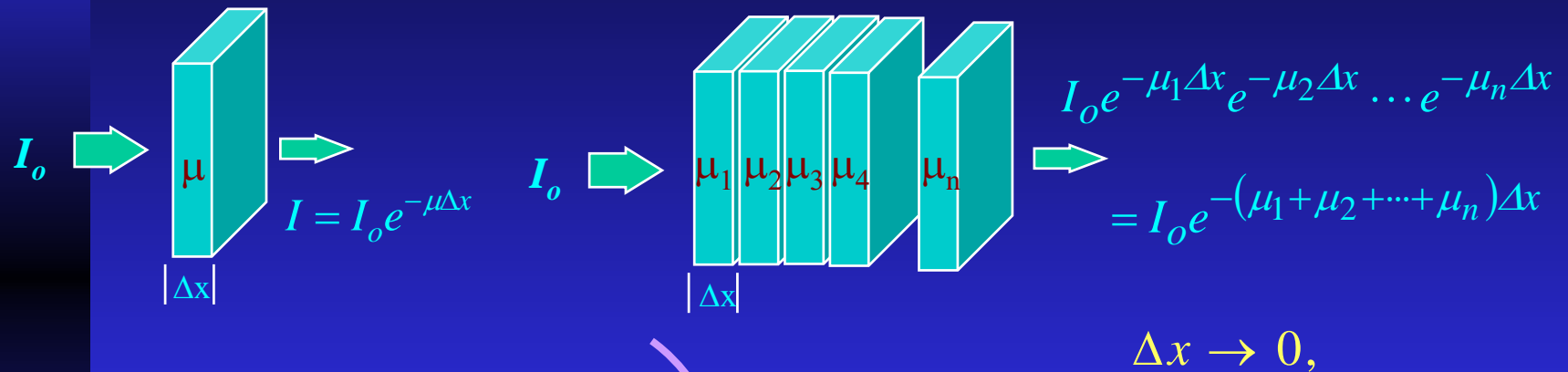
“Textbook” Reconstruction

- The mathematical foundation of CT can be traced back to 1917 to Radon.
- The algorithms can be classified into two classes: analytical and iterative.
- Some of the commonly used reconstruction formulae were developed in the late 70s and early 80s.
- With the introduction of multi-slice helical CT, new cone beam reconstruction algorithms become the focus of research area.

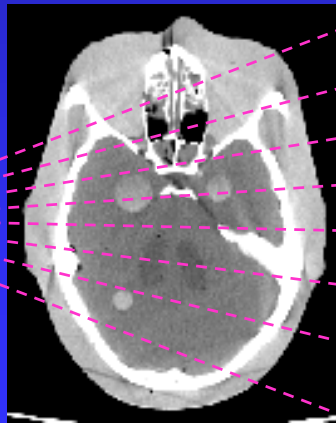
CT Data Measurement

-Under Ideal Conditions

- x-ray attenuation follows Beer's law.



x-ray tube



detector

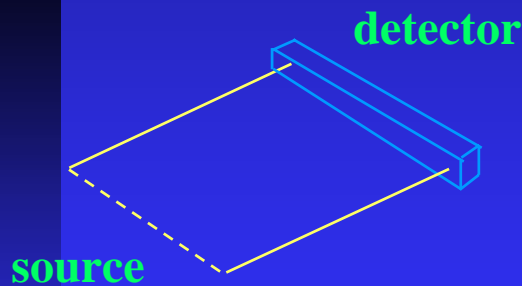
$$P = -\ln \left(\frac{I}{I_o} \right) = \int_{-\infty}^{\infty} \mu(x) dx$$

Measured Projections

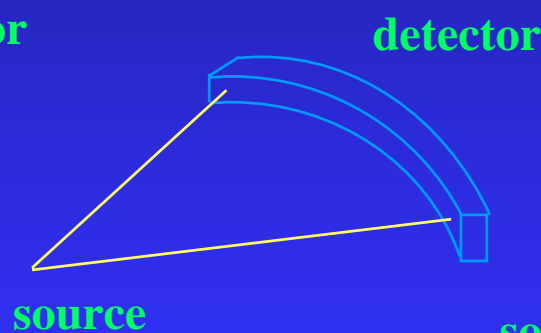
- The measured data are not line integrals of attenuation coefficients of the object.
 - ◆ beam hardening
 - ◆ scattered radiation
 - ◆ detector and data acquisition non-linearity
 - ◆ patient motion
 - ◆ others
- The data need to be calibrated prior to the tomographic reconstruction to obtain artifact-free images.

Sampling Geometries

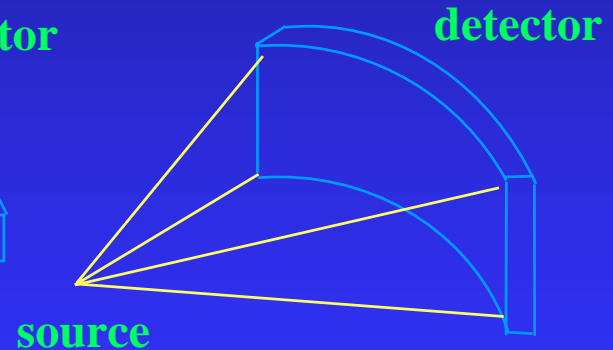
- The sampling geometry of CT scanners can be described three configurations.
- Due to time constraints, we will not present in-depth discussions on each geometry.



parallel beam



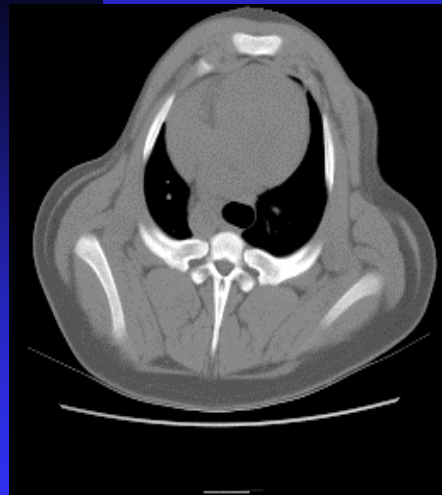
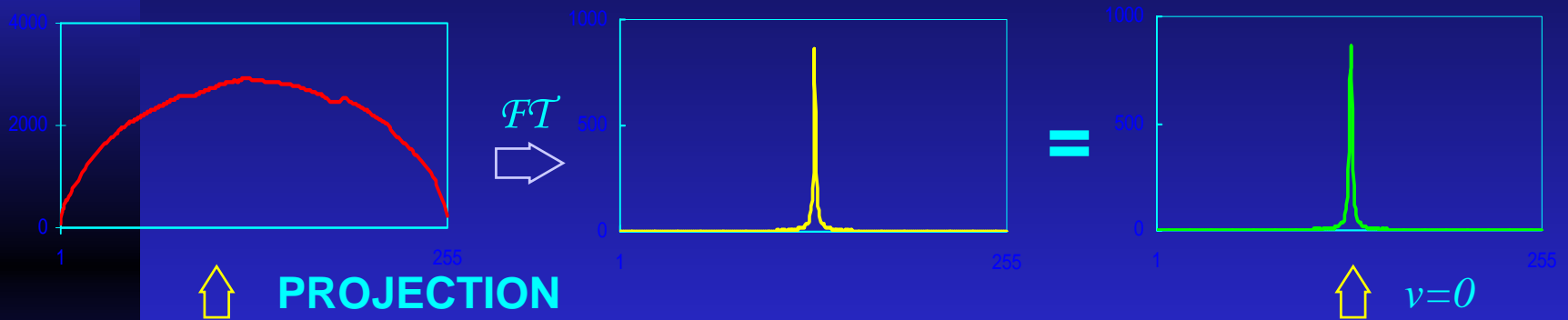
fan beam



cone beam

Fourier Slice Theorem (Central Slice Theorem)

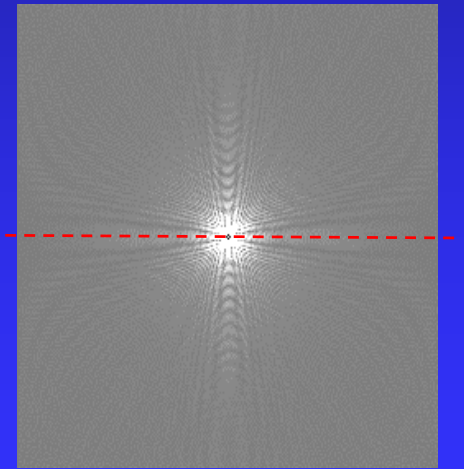
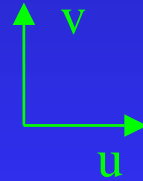
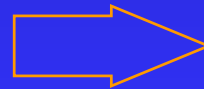
$$p_0(x) = \int_{-\infty}^{\infty} f(x, y) dy \quad P_0(u) = \int_{-\infty}^{\infty} \int_{-\infty}^{\infty} f(x, y) e^{-i2\pi ux} dx dy \quad P(u, 0) = \int_{-\infty}^{\infty} \int_{-\infty}^{\infty} f(x, y) e^{-i2\pi ux} dx dy$$



$f(x, y)$



2D FT

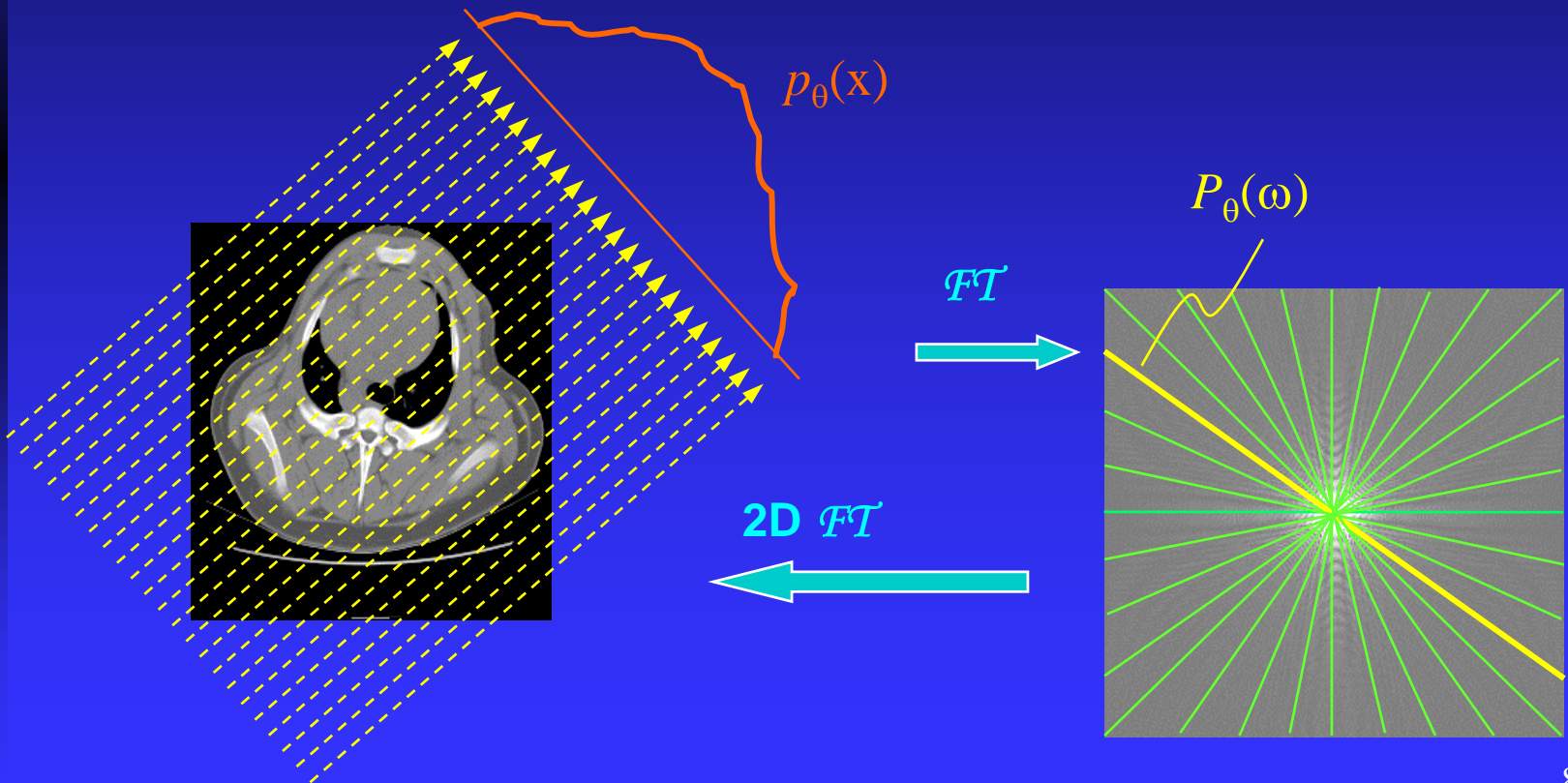


$$F(u, v) = \int_{-\infty}^{\infty} \int_{-\infty}^{\infty} f(x, y) e^{-i2\pi(ux+vy)} dx dy$$

Fourier Slice Theorem

(central slice theorem)

- Fourier transform of projections at different angles fill up the Fourier space.
- Inverse Fourier transform recovers the original object.

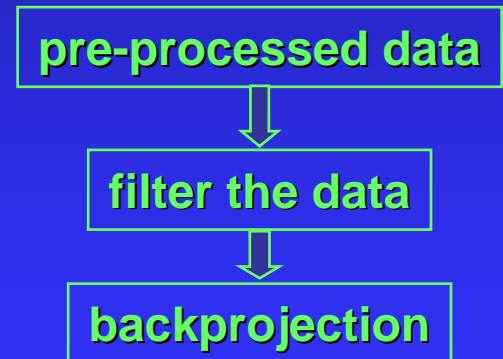
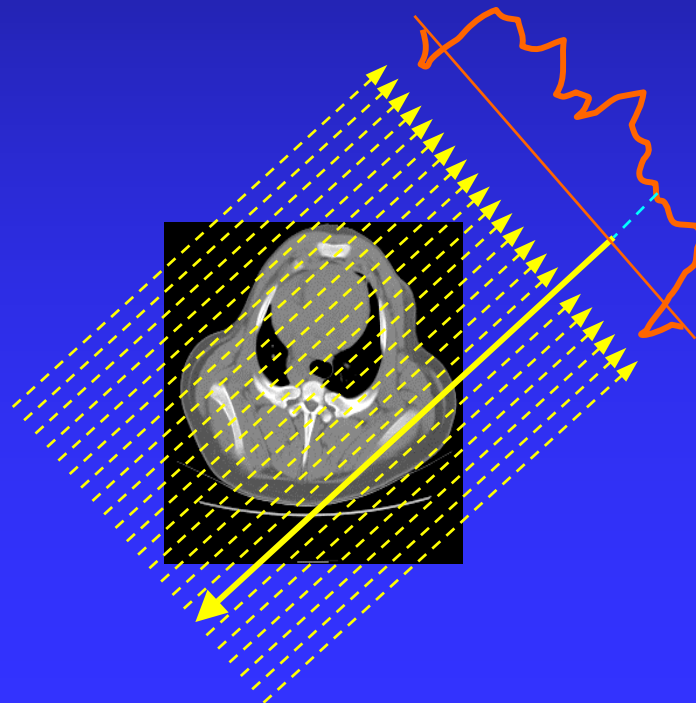
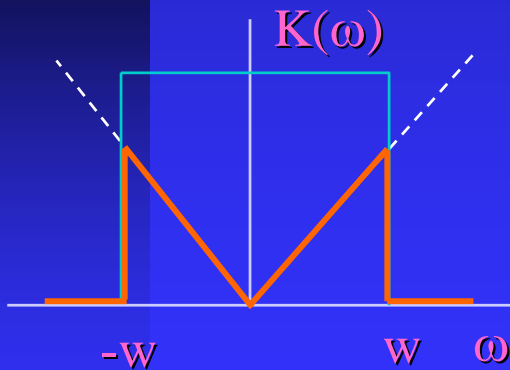


Filtered Backprojection

- The filtered backprojection formula can be derived from the Fourier transform pair, coordinate transformation, and the Fourier slice theory:

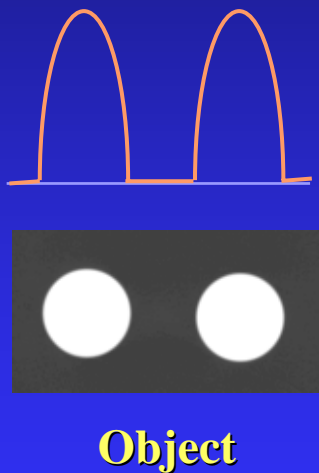
$$f(x, y) = \int_0^\pi \int_{-\infty}^{\infty} P_\theta(\omega) |\omega| e^{j2\pi\omega t} d\omega d\theta$$

backprojection
filtering



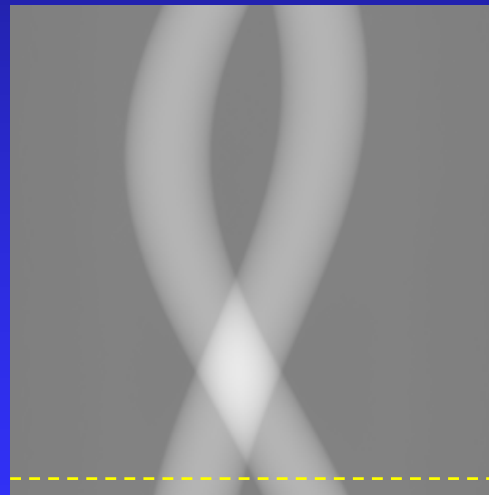
Filtering

- Consider an example of reconstructing a phantom object of two rods.



views

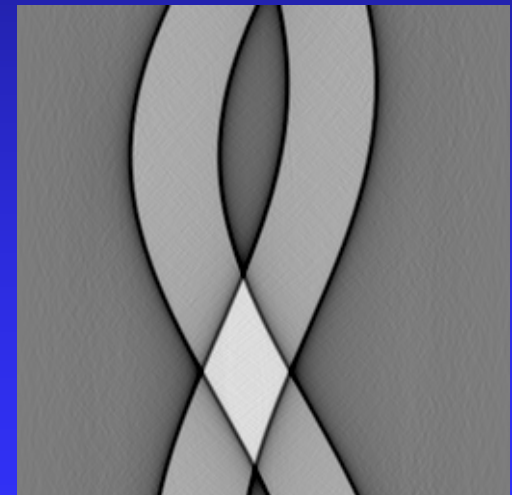
Original Sinogram



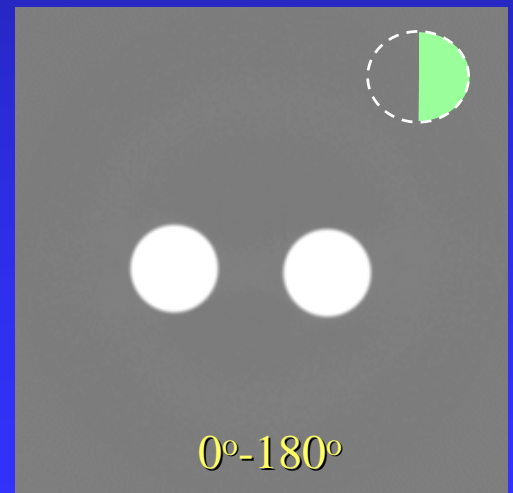
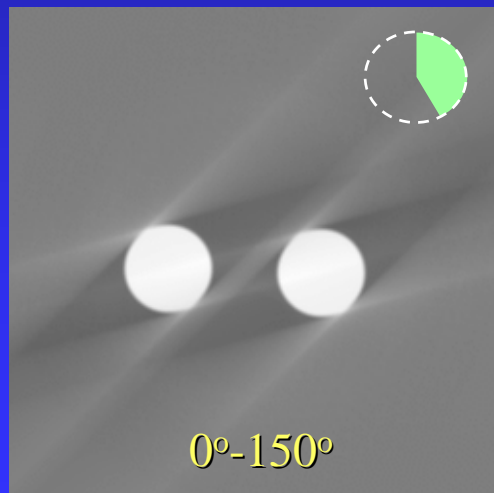
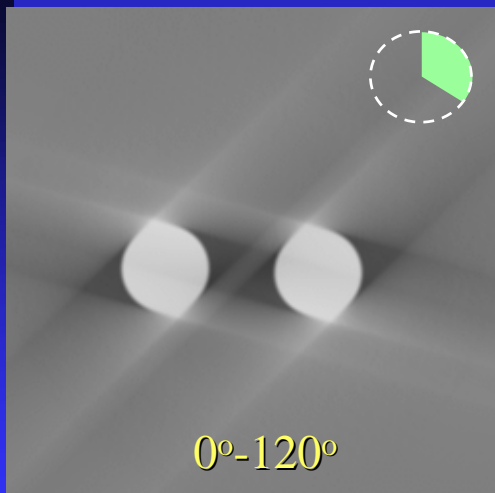
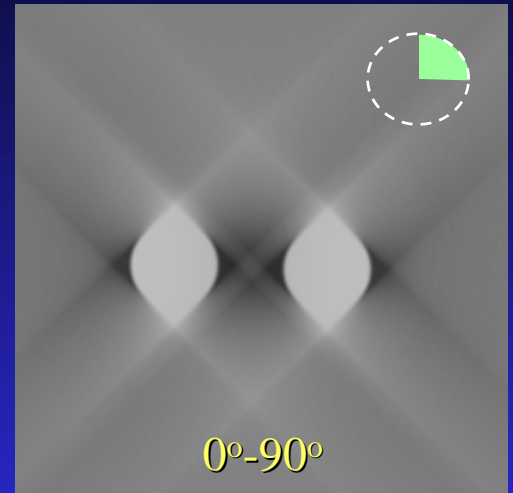
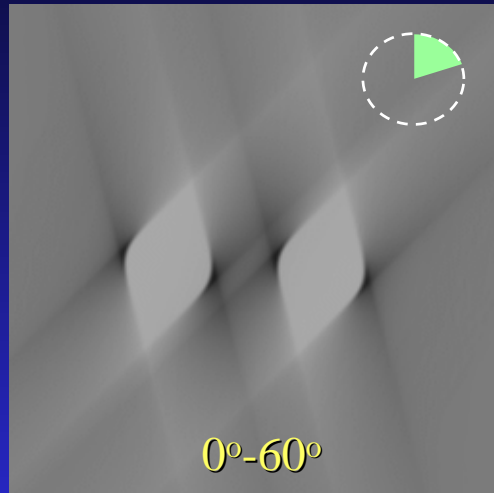
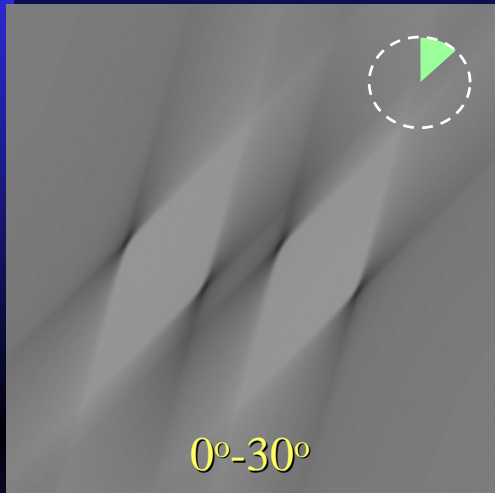
single
projection

detector sample

Filtered Sinogram

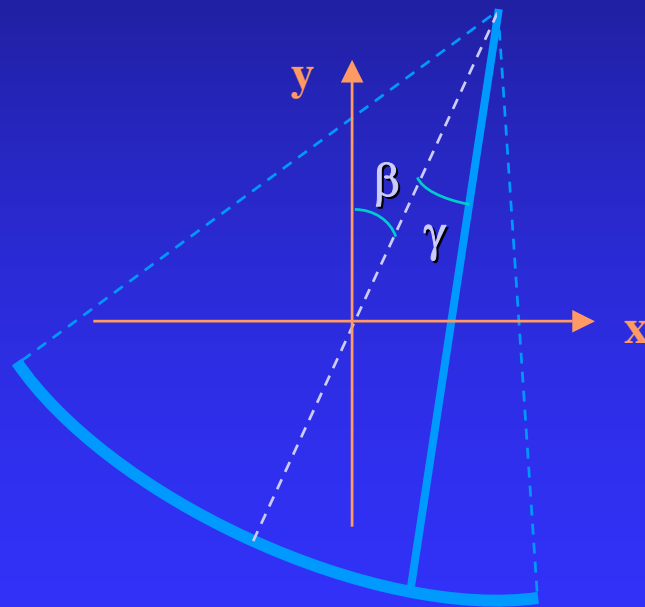


Backprojection

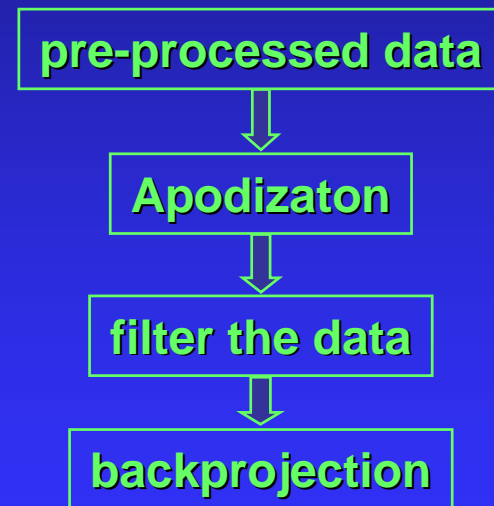


Fan Beam Reconstruction

- Each ray in a fan beam can be specified by β and γ .
- Reconstruction process is similar to parallel reconstruction except additional “apodization” step and weighting in the backprojection.



fan beam geometry



fan beam reconstruction

Equiangular Fan Beam Reconstruction

$$f(x, y) = \int_0^{2\pi} L^{-2} d\beta \int_{-\gamma_m}^{\gamma_m} D \cos \gamma \cdot p(\gamma, \beta) h(\gamma' - \gamma) d\gamma$$

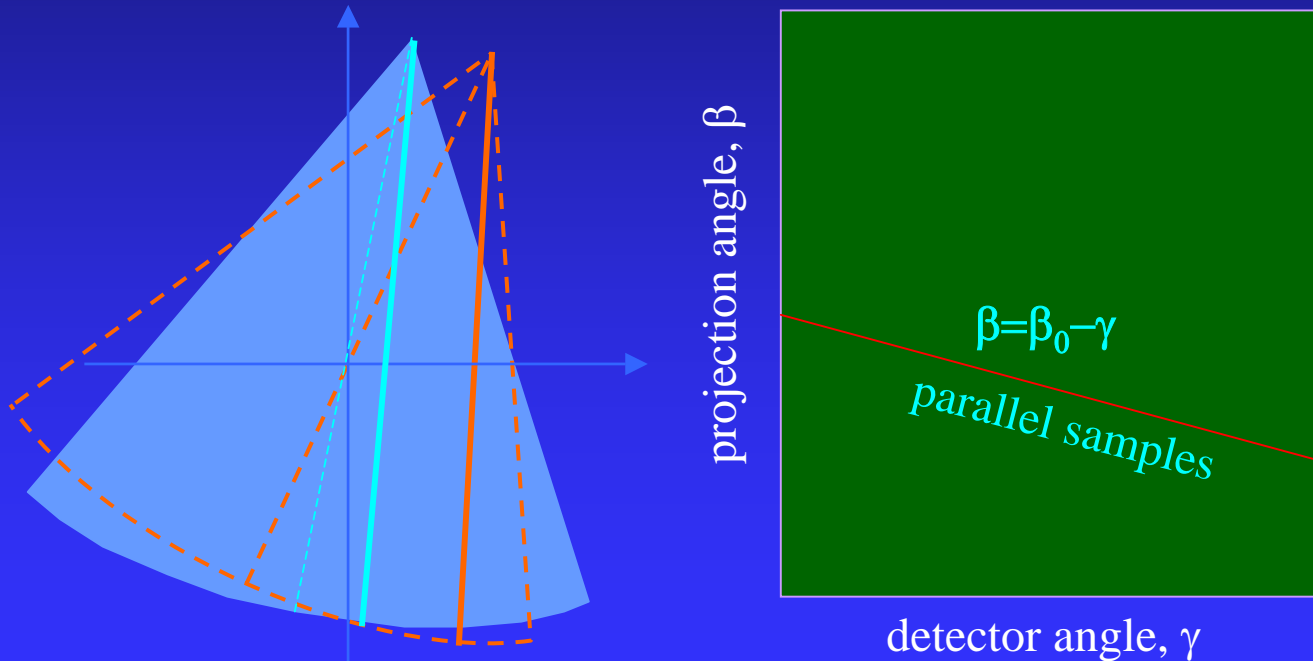
backprojection

filtering

- The projection is first multiplied by the cosine of the detector angle.
- Filtering is applied across detector channels in a similar fashion as the parallel beam reconstruction.
- In the backprojection process, the filtered sample is scaled by the distance to the source.
- Because of the distance-dependent weighting in the backprojection, impact on computation and noise result.

Fan-Para Reconstruction

- Alternatively, the fan beam data can be converted to a set of parallel samples. Parallel reconstruction algorithms can be used for image formation.

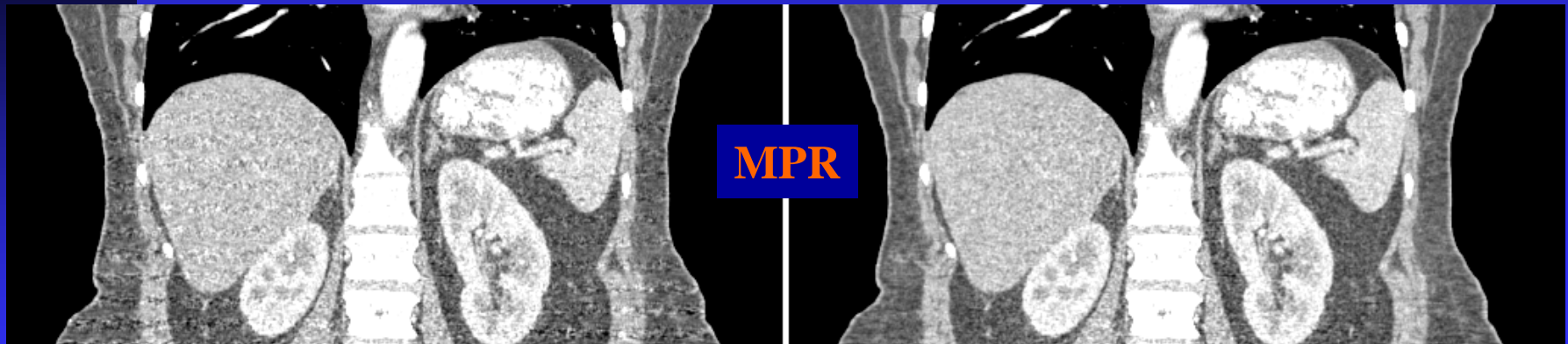


MIP & MPR Image Comparison



fan beam backprojection

parallel beam backprojection



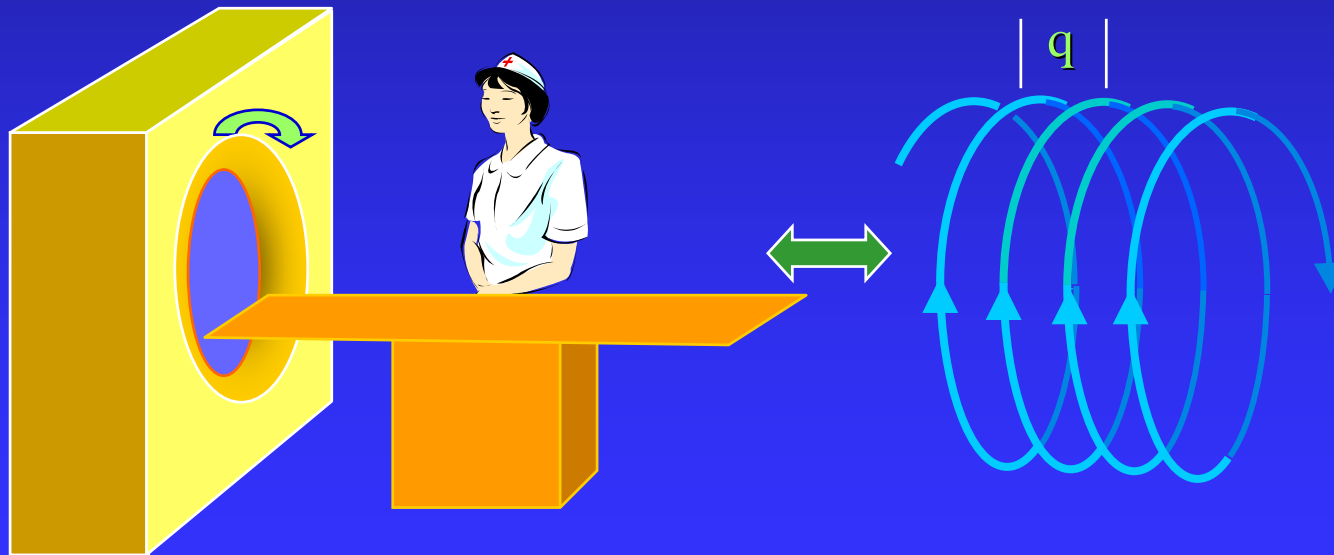
fan beam backprojection

parallel beam backprojection

Helical Scanning

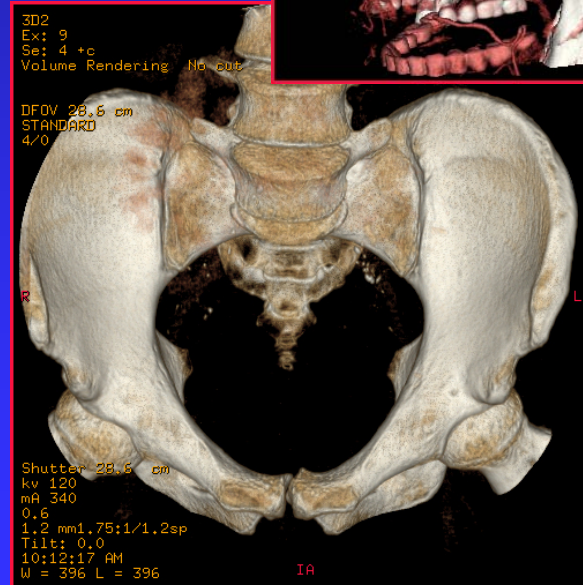
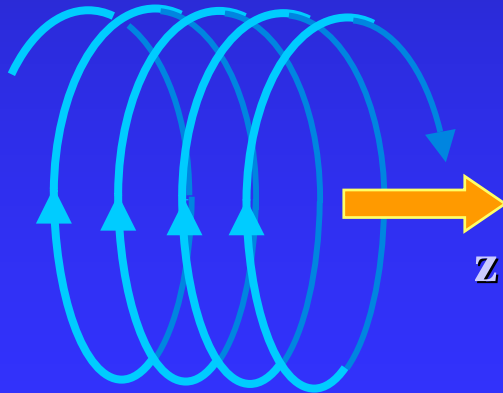
- In helical scanning, the patient is translated at a constant speed while the gantry rotates.
- Helical pitch:

$$h = \frac{q}{d} \quad \begin{array}{l} \text{— distance gantry travel in one rotation} \\ \text{— collimator aperture} \end{array}$$



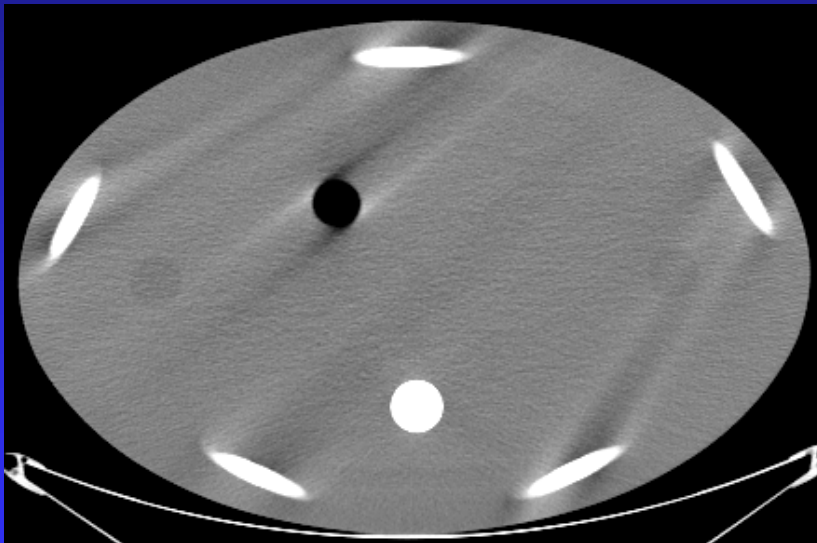
Helical Scanning

- Advantages of helical scanning
 - ◆ nearly 100% duty cycle (no inter-scan delay)
 - ◆ improved contrast on small object (reconstruction at any z location)
 - ◆ improved 3D images (overlapped reconstruction)

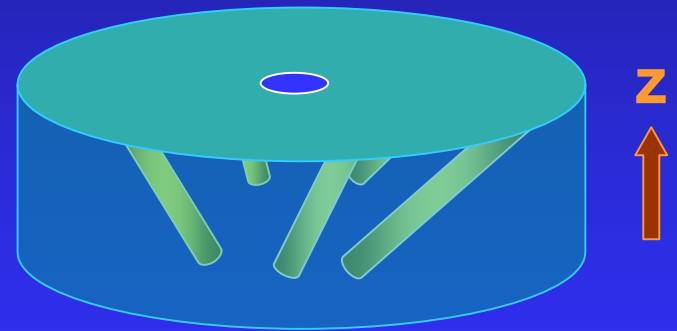


Helical Scanning

- The helical data collection is inherently inconsistent. If proper correction is not rendered, image artifact will result.

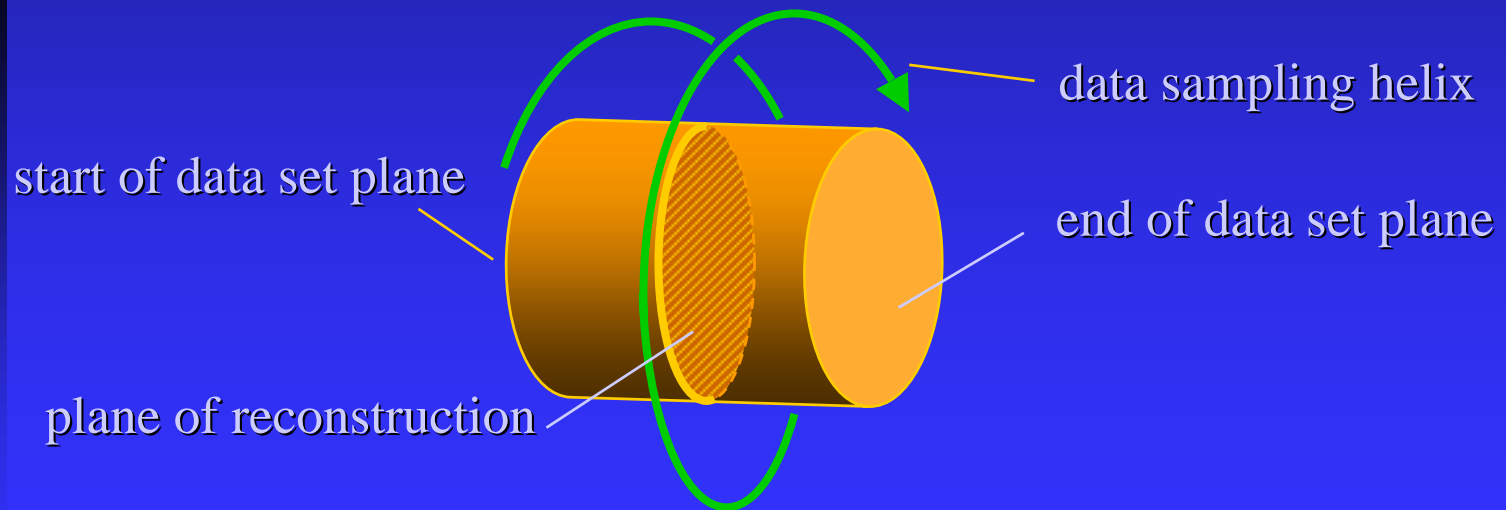


**reconstructed helical
scan without correction**



Helical Reconstruction

- The plane of reconstruction is typically at the mid-point between the start and end planes.
- Interpolation is performed to estimate a set of projections at the plane of reconstruction.



Helical Reconstruction

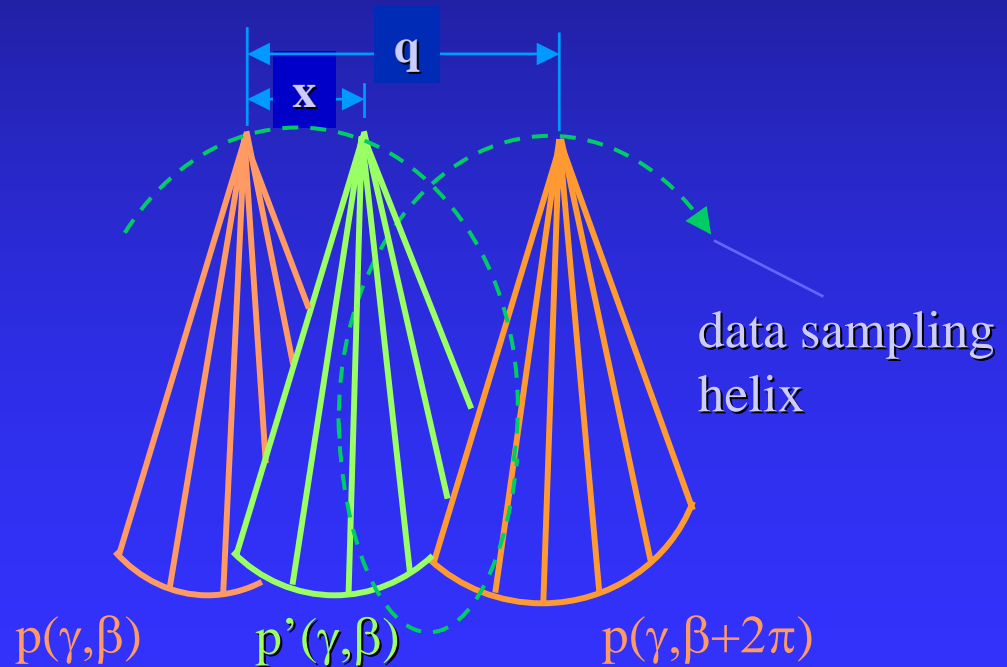
-360° interpolation

- Samples at the plane-of-reconstruction is estimated using two projections that are 360° apart.

$$p'(\gamma, \beta) = wp(\gamma, \beta) + (1 - w)p(\gamma, \beta + 2\pi)$$

where

$$w = \frac{q - x}{q}$$



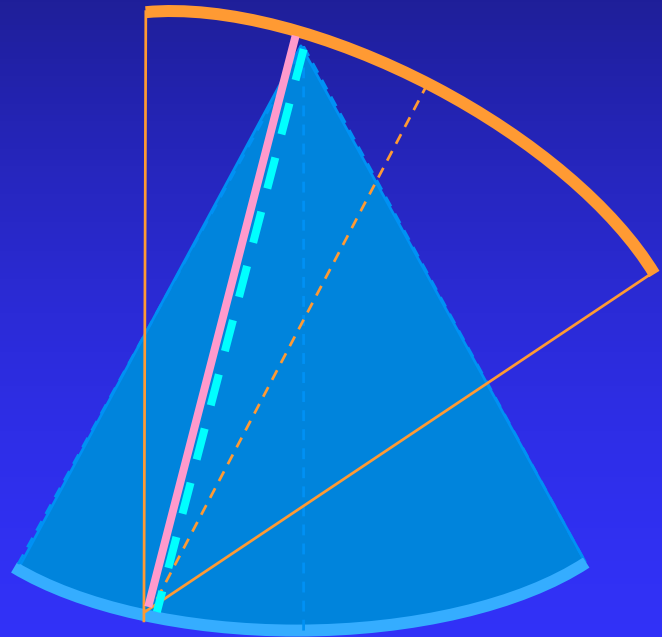
Helical Reconstruction

-180° interpolation

- In fan beam, each ray path is sampled by two conjugate samples that are related by:

$$\begin{cases} \gamma' = -\gamma \\ \beta' = \beta + \pi + 2\gamma \end{cases}$$

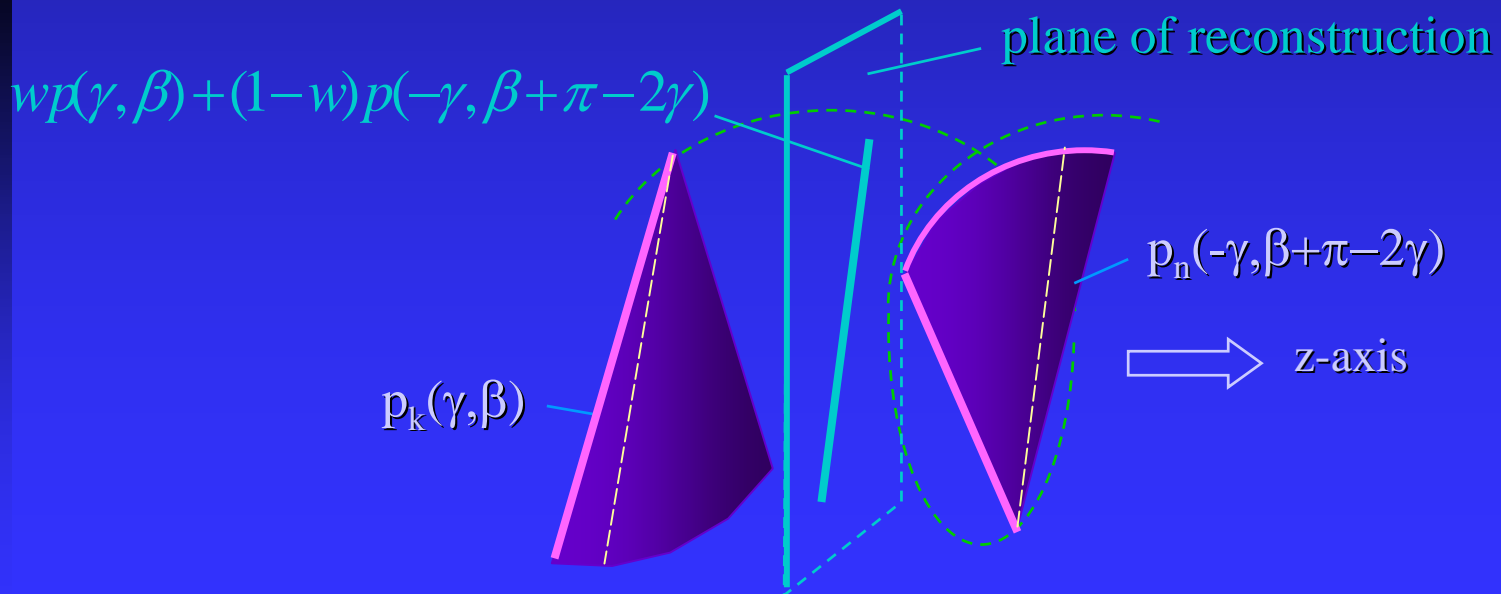
For helical scan, these two samples are taken at different z location because of the table motion.



Helical Reconstruction

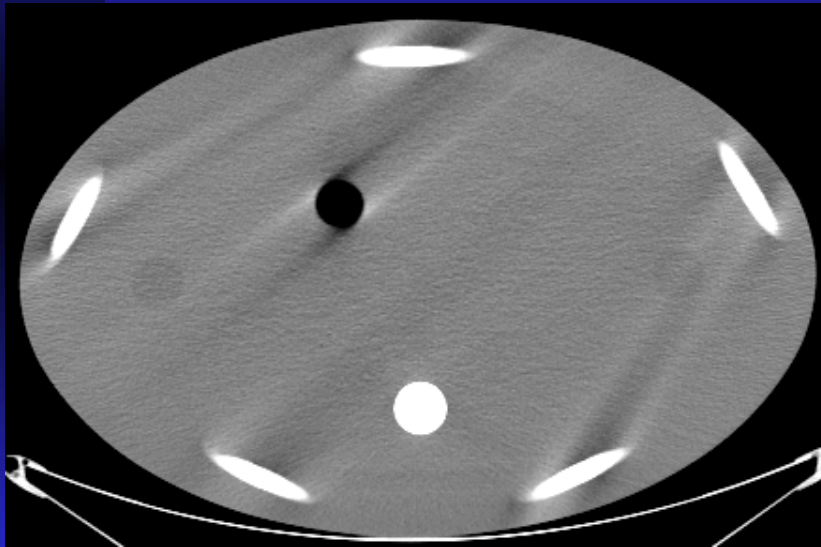
-180° interpolation

- Linear interpolation is used to estimate the projection samples at the plane of reconstruction.
- Because samples are taken at different view angles, the weights are γ - and β -dependent.

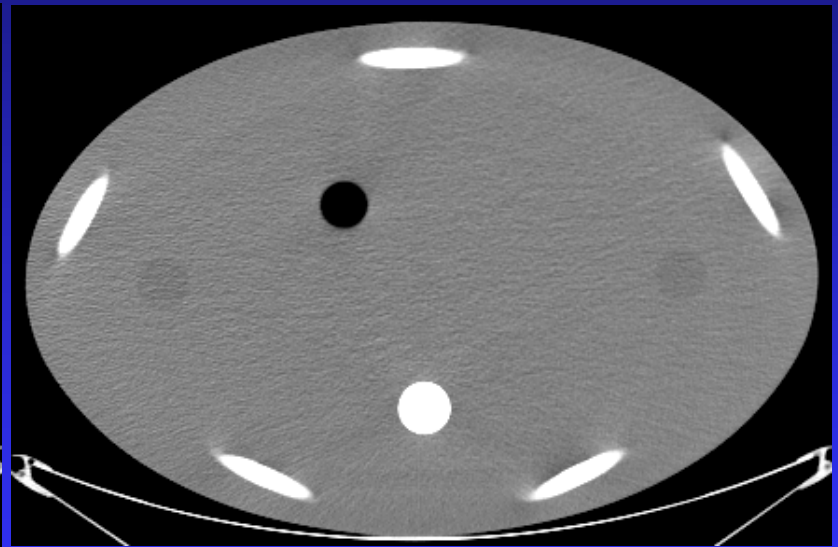


Artifact Suppression

- Helical reconstruction algorithm effectively suppresses helical artifacts.



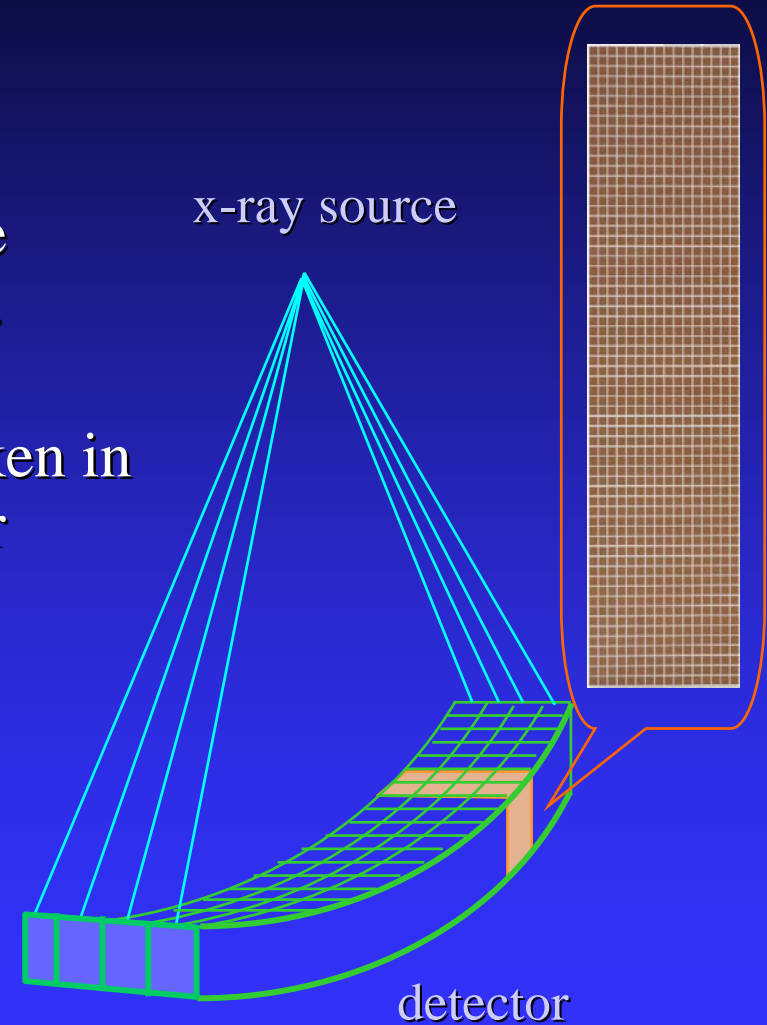
without helical correction



with helical correction

Multi-slice CT

- Multi-slice CT contains multiple detector rows.
- For each gantry rotation, multiple slices of projections are acquired.
- Similar to the single slice configuration, the scan can be taken in either the step-and-shoot mode or helical mode.

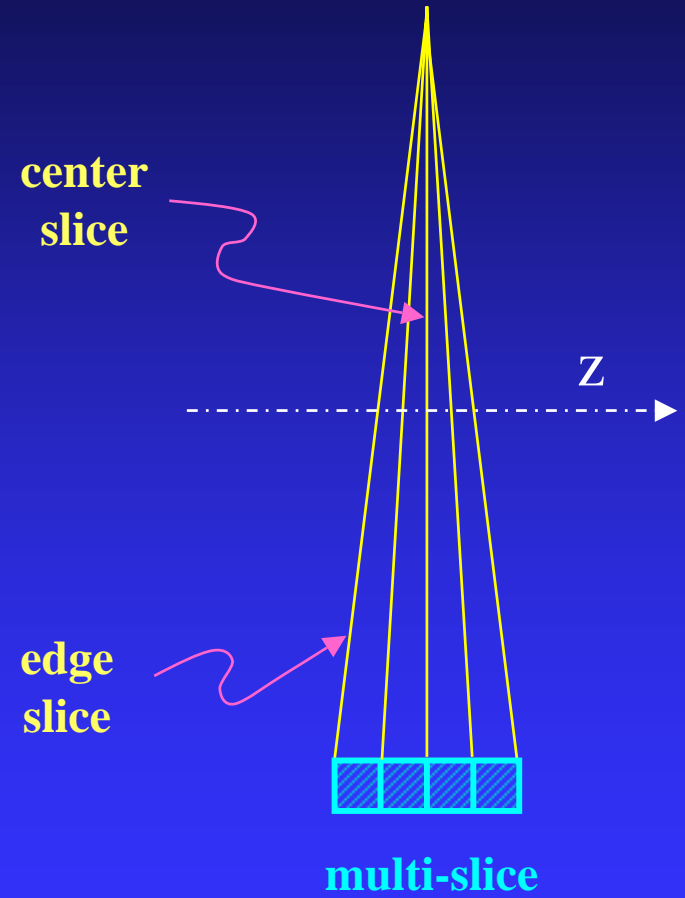
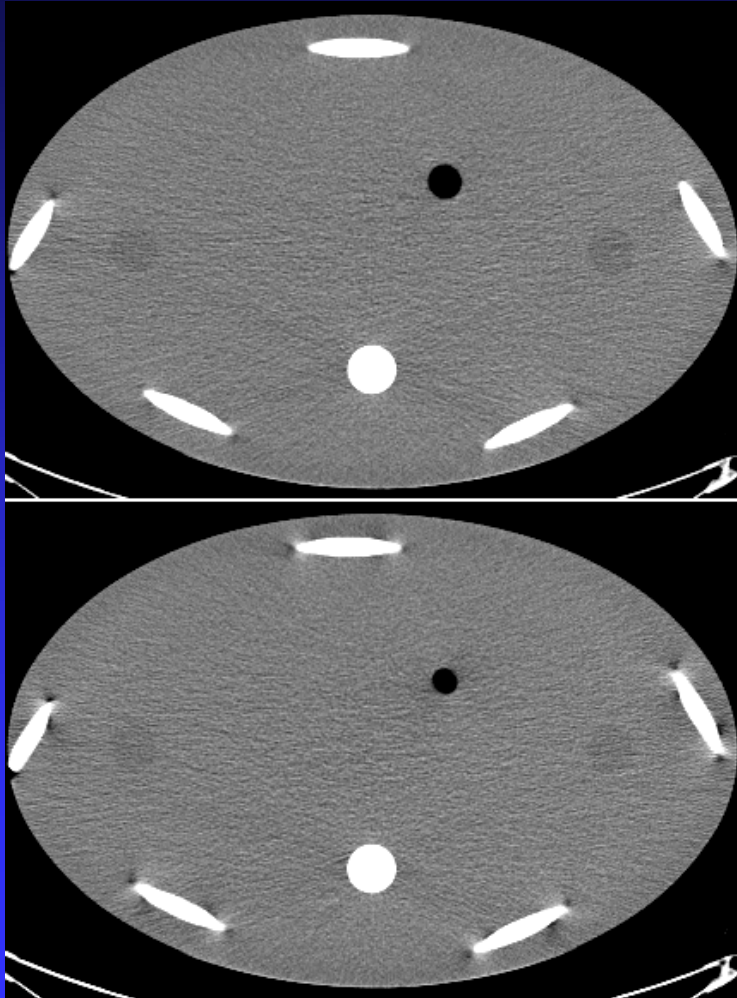


Advantages of Multi-slice

- Large coverage and faster scan speed
- Better contrast utilization
- Less patient motion artifacts
- Isotropic spatial resolution



Cone Beam Artifact

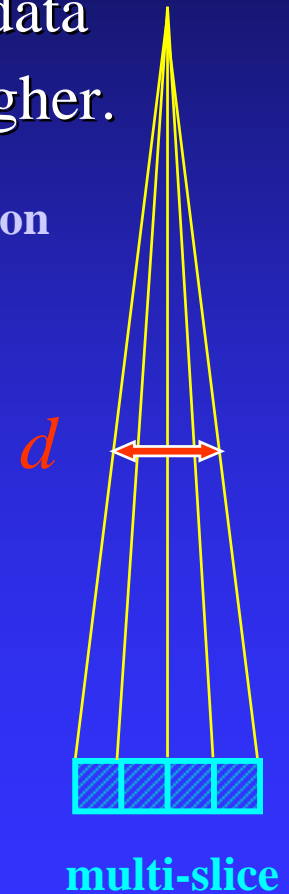
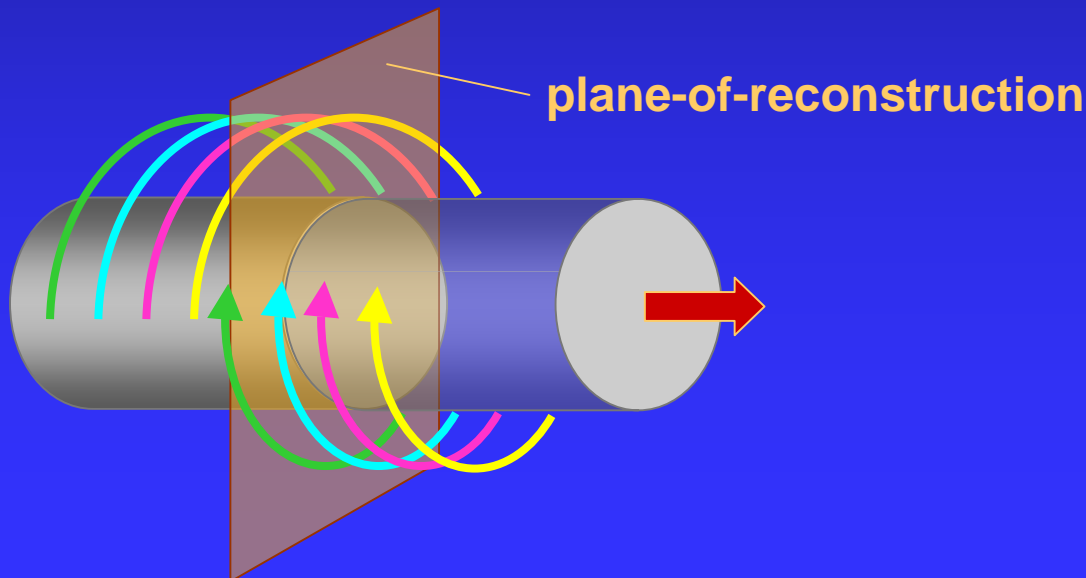


Multi-slice Helical

- When acquiring data in a helical mode, the N detector rows form N interweaving helices.
- Because multiple detector rows are used in the data acquisition, the acquisition speed is typically higher.

$$h = \frac{q}{d}$$

— distance gantry travel in one rotation
— collimator aperture



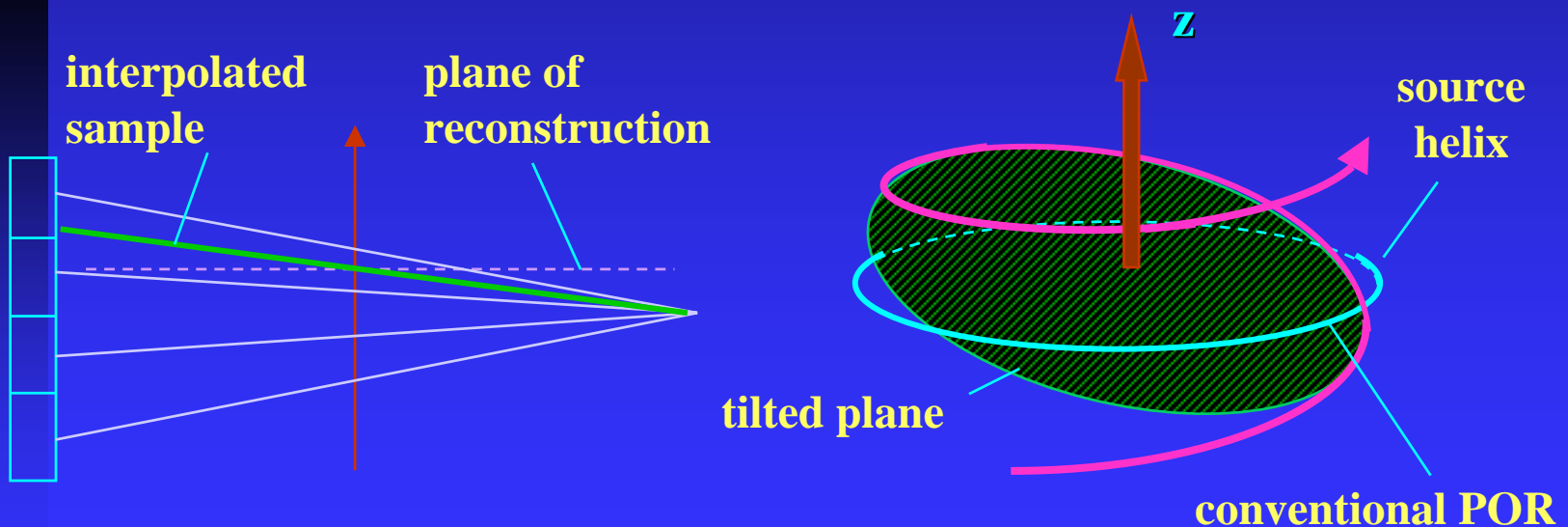
Cone Beam Helical Reconstruction

- Exact algorithms produce mathematically exact solutions when input projections are perfect.
 - ◆ Katsevich
 - ◆ Grangeat
 - ◆ Rebin PHI
 - ◆ FBP PHI
- Approximate algorithms, although non-exact, generate clinically accurate images.
 - ◆ FDK-type
 - ◆ N-PI
 - ◆ CB-virtual circle
 - ◆ Tilted Plane
 - ◆ ZB
- Generally speaking, approximate algorithms are computationally less expensive and more flexible.

Cone Beam Algorithm

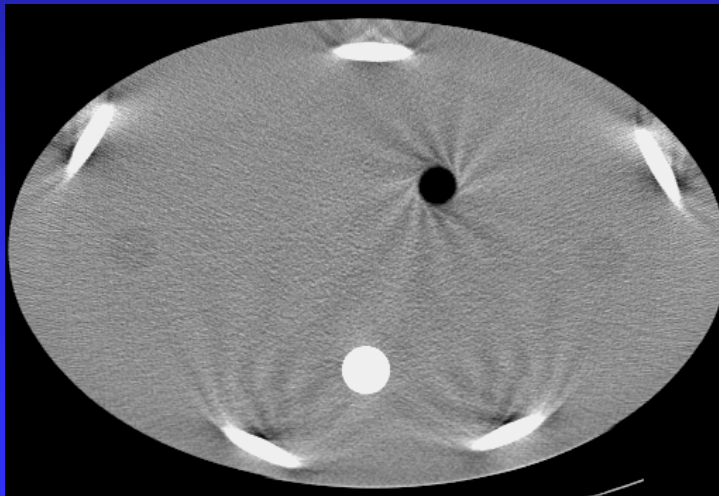
small cone angle

- From a computational point of view, 3D backprojection is more expensive than 2D backprojection.
- To reduce computation, reconstruction planes are defined as planes that best fit the helix so that 2D reconstruction algorithm can still be used.

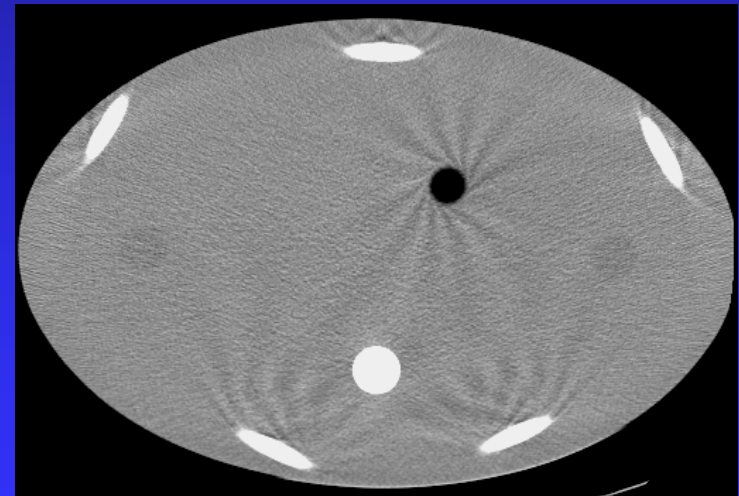


Tilted Plane Reconstruction

- For small cone angles, the flat plane and source helix match quite well.
- When the same weighting function is used, reconstructions with the tilted plane produces better image quality than the conventional reconstruction plane with 2D backprojection.



conventional plane

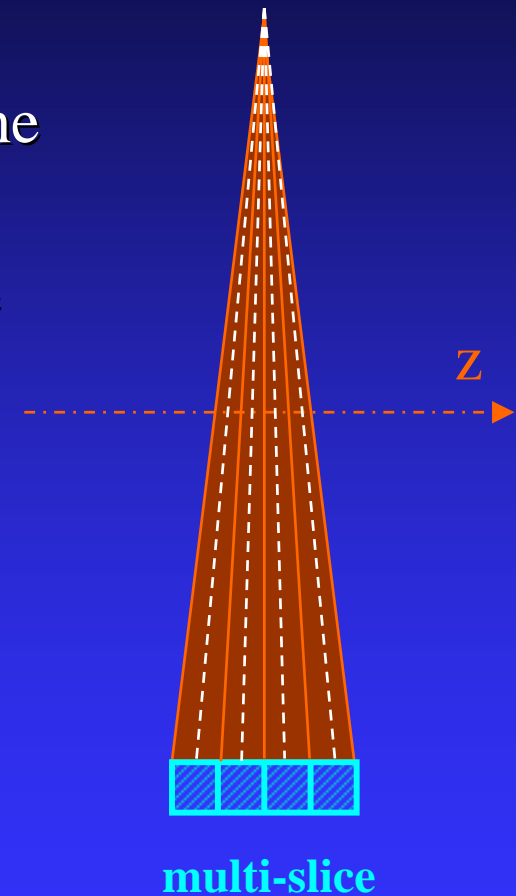
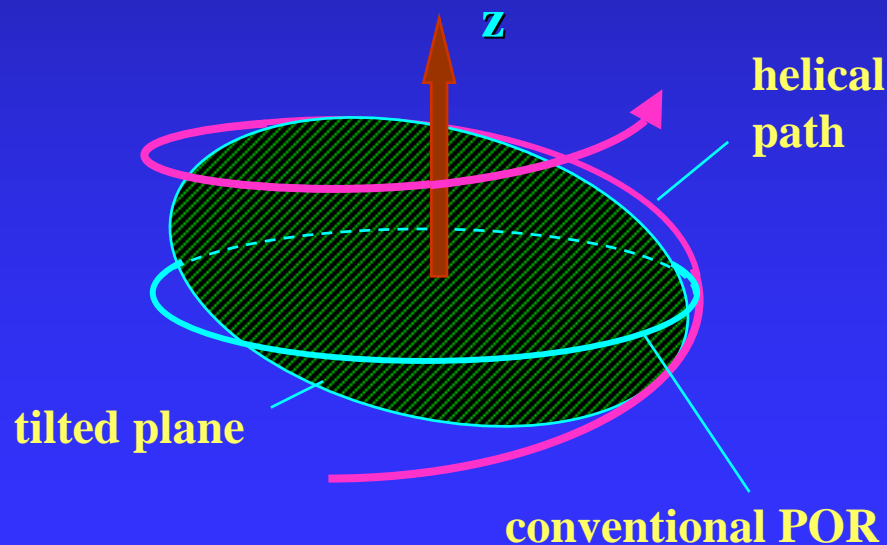


tilted plane

Cone Beam Reconstruction

moderate cone angle

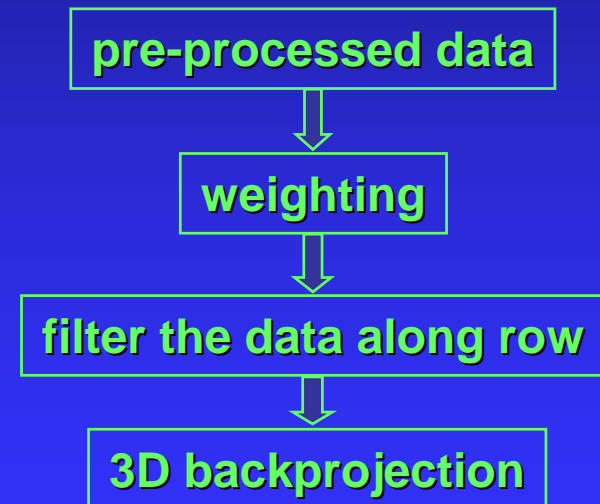
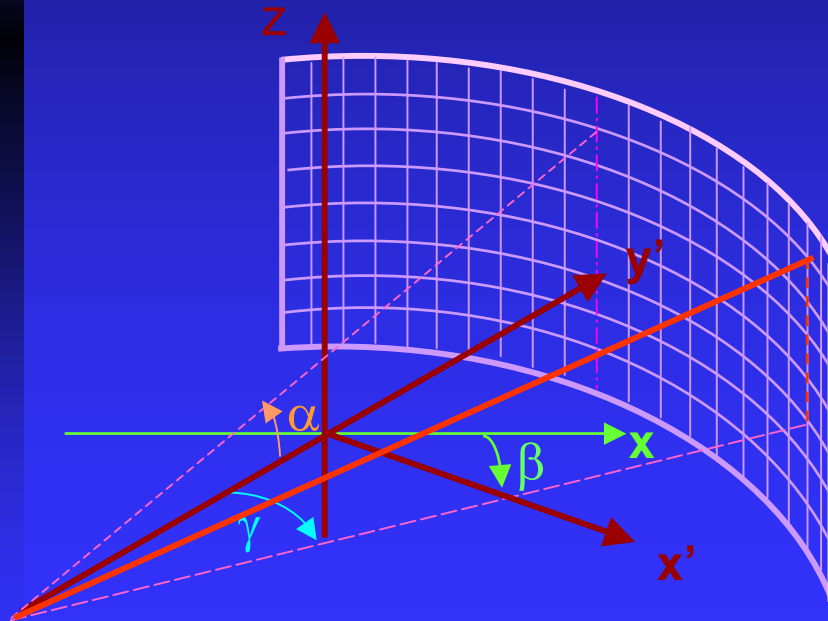
- For larger cone angles, tilted plane reconstruction is no longer sufficient, due to the larger difference between the flat plane and the curved helix.
- FDK-type algorithm with appropriate weighting is often used.



Cone Beam Reconstruction

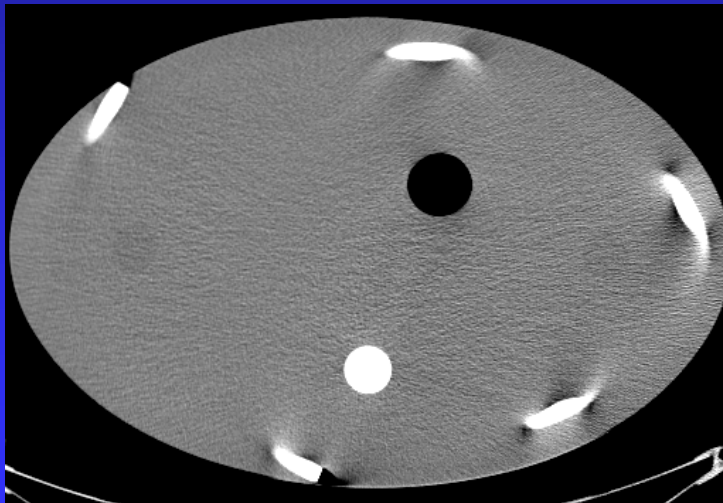
FDK Algorithm

- Each ray in a cone beam can be specified by β , γ , and α .
- FDK algorithm was derived from fan-beam algorithm by studying the impact of cone angle to the rotation angle.
- Unlike parallel or fan beam algorithms, FDK algorithm is an approximation.

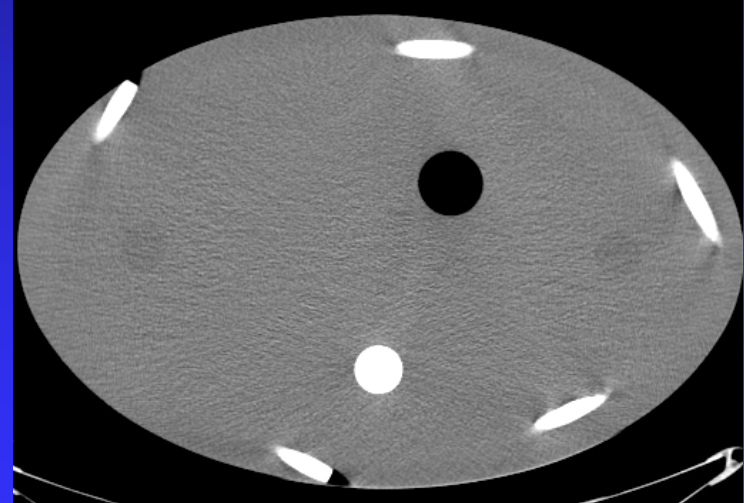


FDK-type Algorithm

- FDK-type algorithm can be combined with different weighting functions to optimize its performance in different performance parameters.
- Cone beam artifacts are suppressed but not completely eliminated.



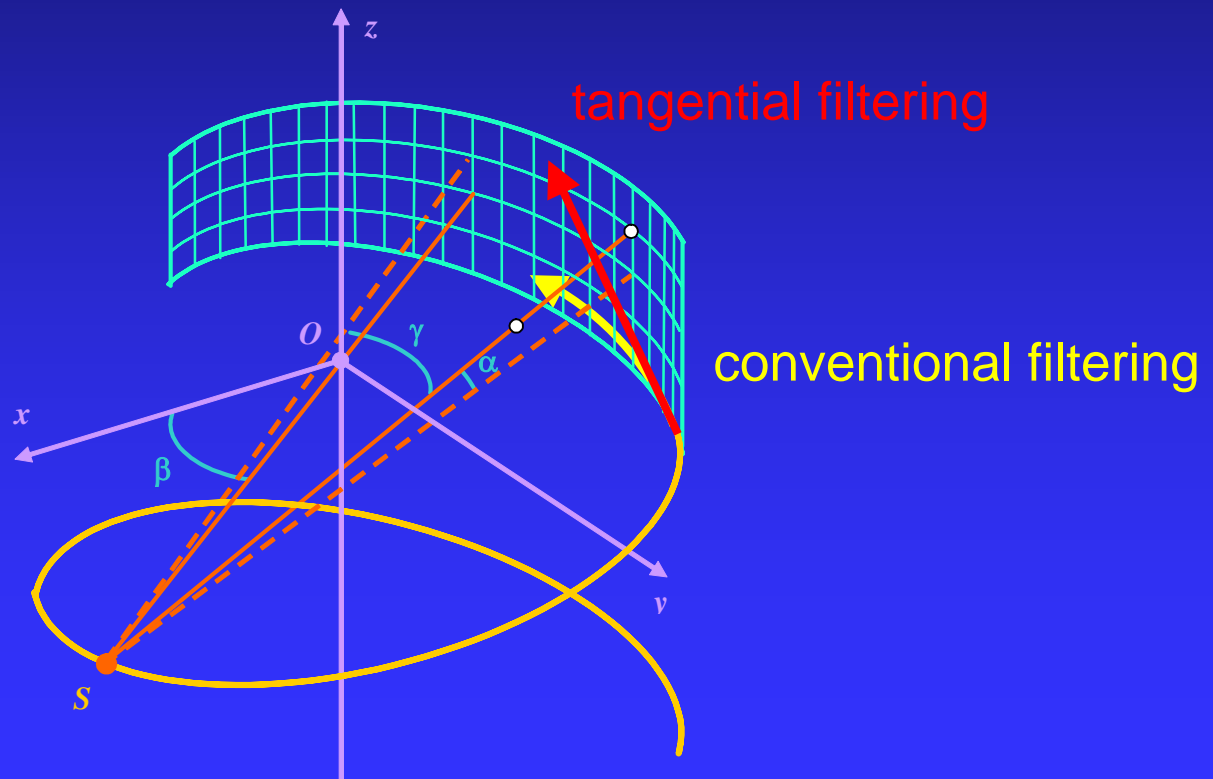
original



FDK-based

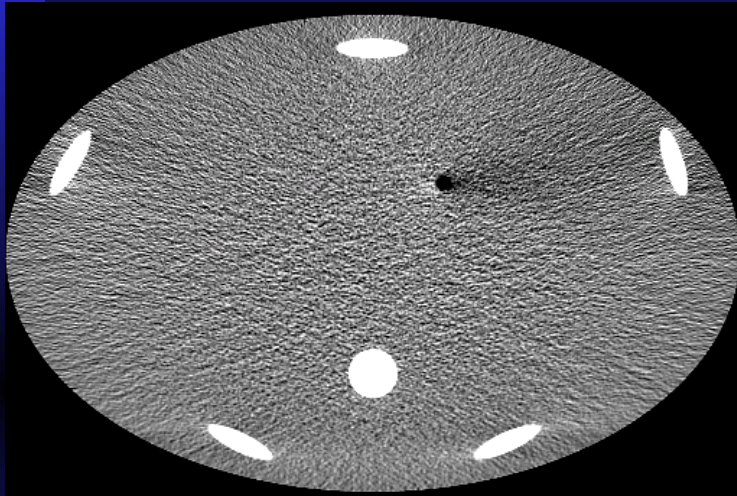
Tangential Filtering

- Conventional filtering process is carried out along detector rows.
- Tangential filtering is carried out along the tangential direction of the source trajectory.

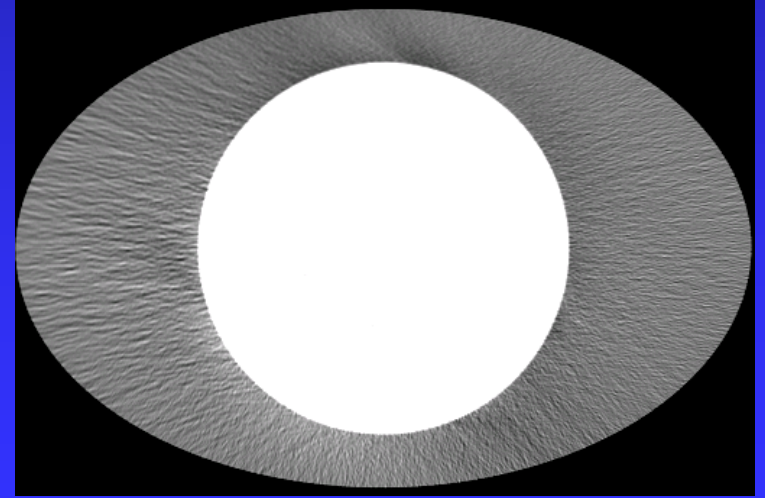
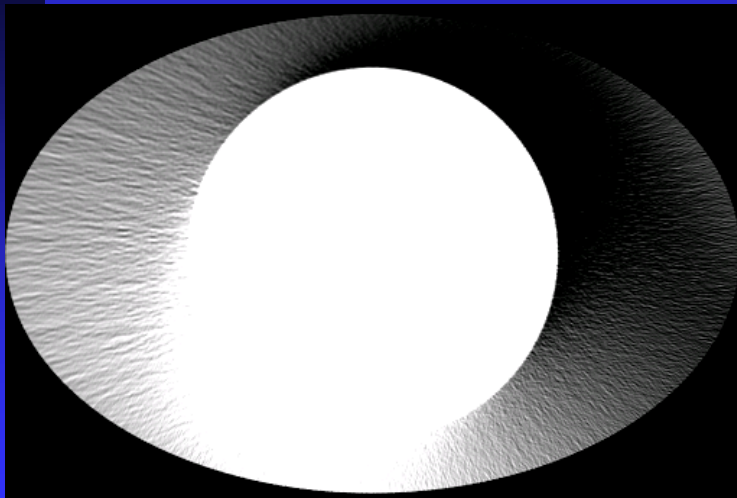
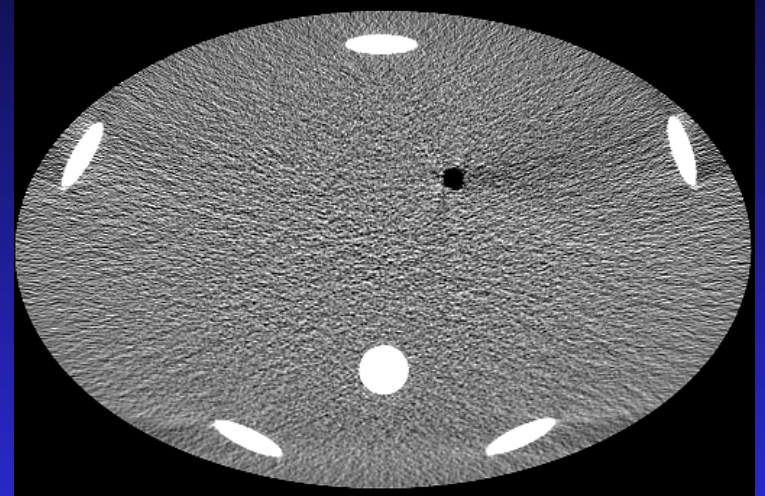


Tangential Filtering

conventional filtering

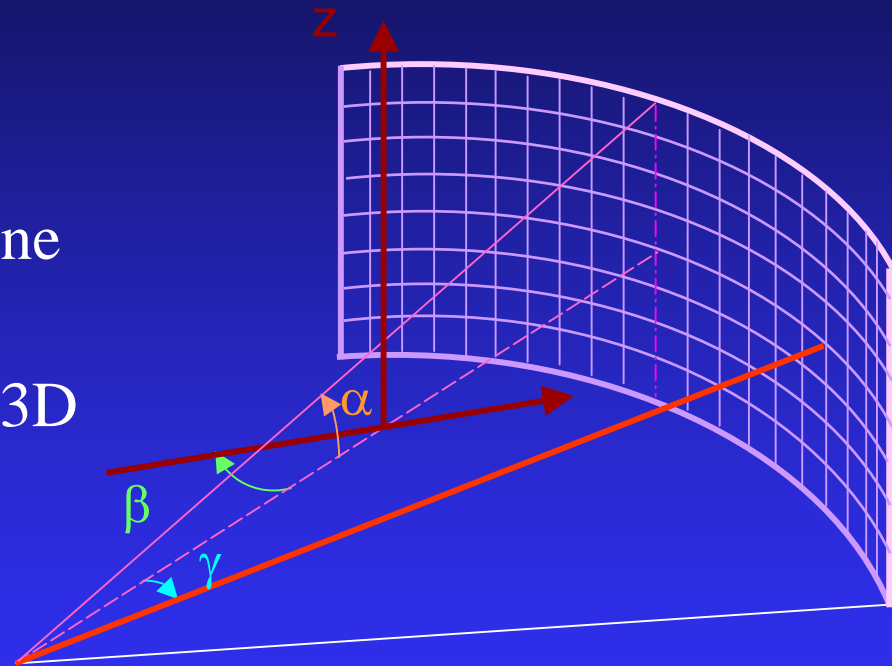


tangential filtering



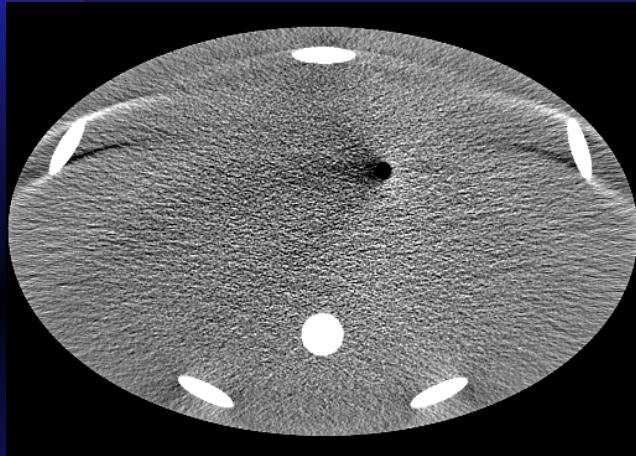
3D Helical Weighting

- The helical weighting function changes with projection angle β , detector angle γ , and cone angle α .
- Experiments show that 3D weighting function provides significant improvement in image quality.

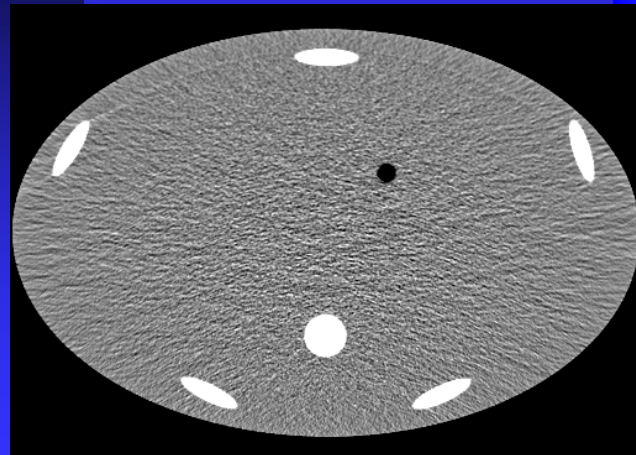
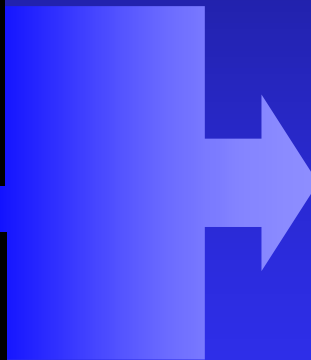


3D Helical Weighting

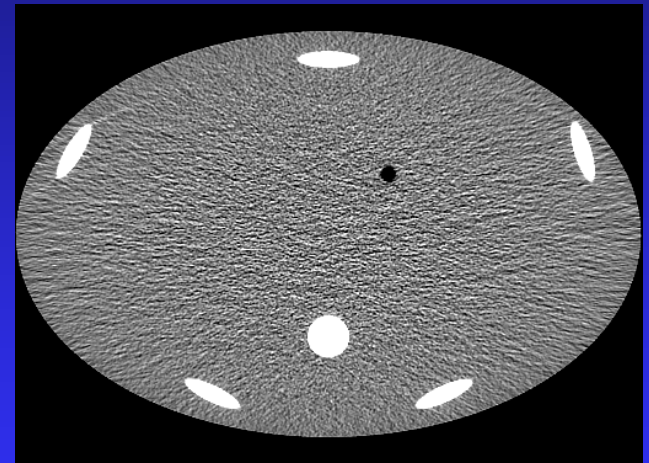
- For moderate cone angle, FDK with 3D weighting can provide equivalent image quality as the exact algorithms.



"off the shelf"
recon



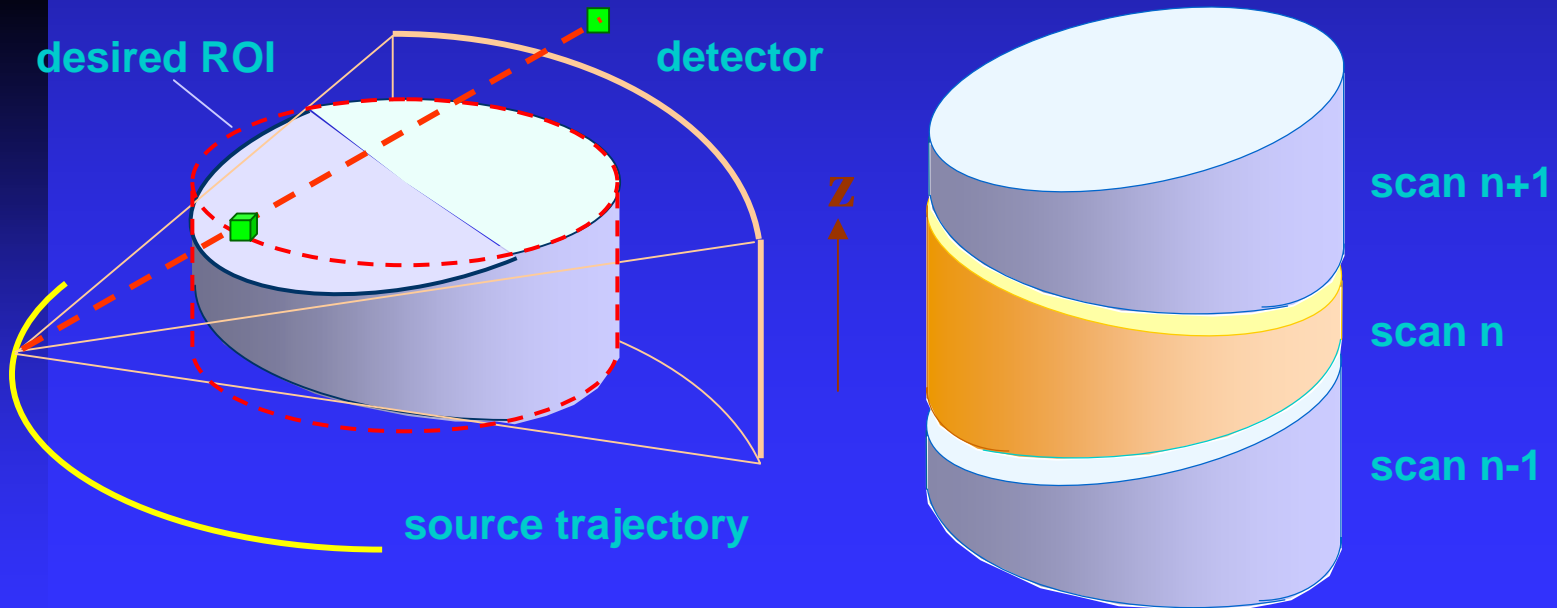
more expensive
exact recon



3D weighting

Reconstruction

- Half-scan ($180^\circ + \text{fan angle}$) for reconstruction
- Volume covered non-uniformly due to cone beam
- Extrapolation to estimate the missing data
- Adjacent scans to provide complimentary information



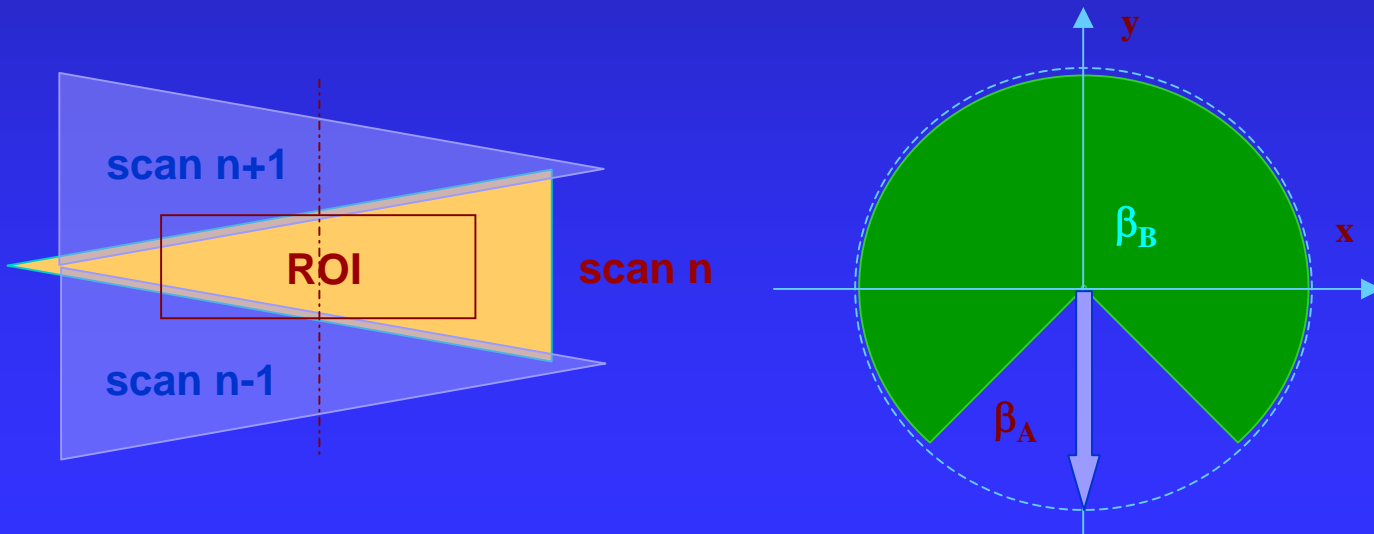
Cone Beam Reconstruction

- For each image voxel, a quality factor is generated based on the amount of extrapolation used in the reconstruction.

$$\eta(x, y, z) = \int_0^{\pi + \gamma_m} \varphi(v, \beta) d\beta$$

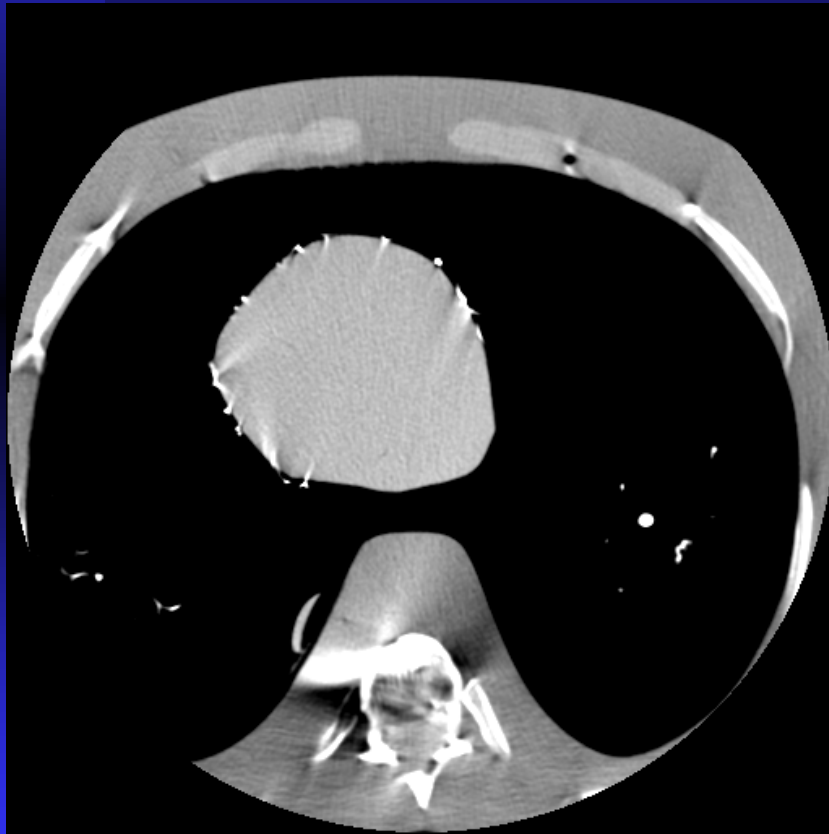
- The final image is the weighted sum of adjacent scans.

$$f(x, y, z) = \frac{\eta_B(x, y, z)}{\eta_A(x, y, z) + \eta_B(x, y, z)} f_A(x, y, z) + \frac{\eta_A(x, y, z)}{\eta_A(x, y, z) + \eta_B(x, y, z)} f_B(x, y, z)$$

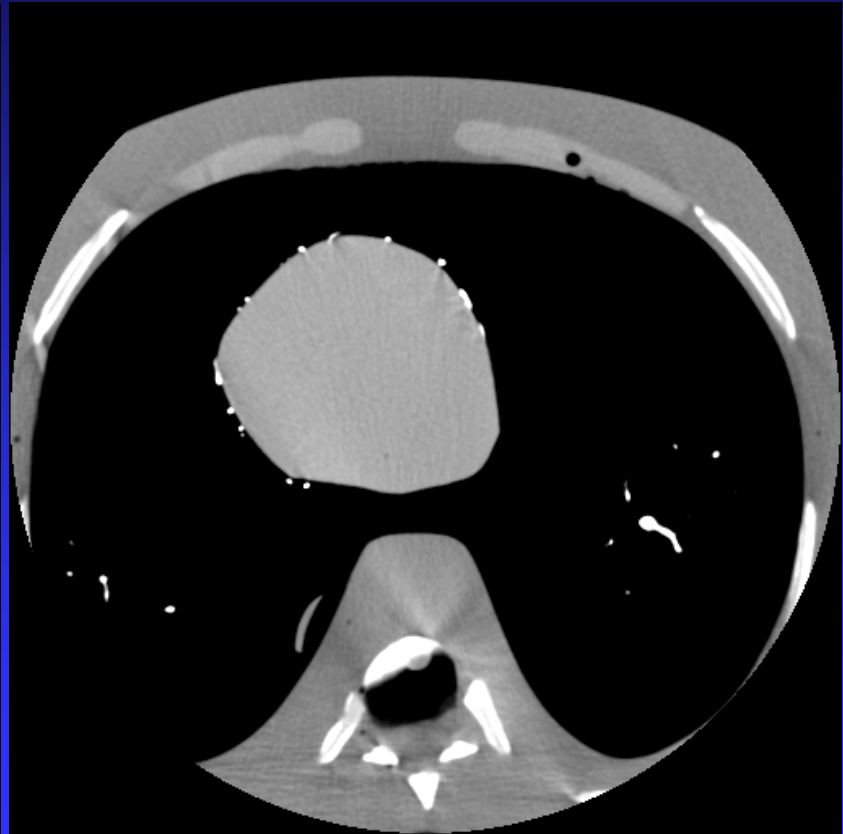


Phantom Results

- Heart phantom scanned on LightSpeed VCT⁶⁴ (64x0.625mm)
- Image for the outer most slice



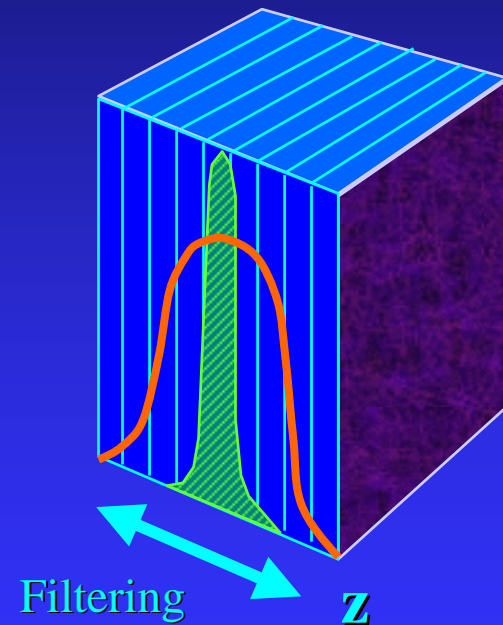
conventional reconstruction



proposed reconstruction

Slice Thickness Change With Algorithm

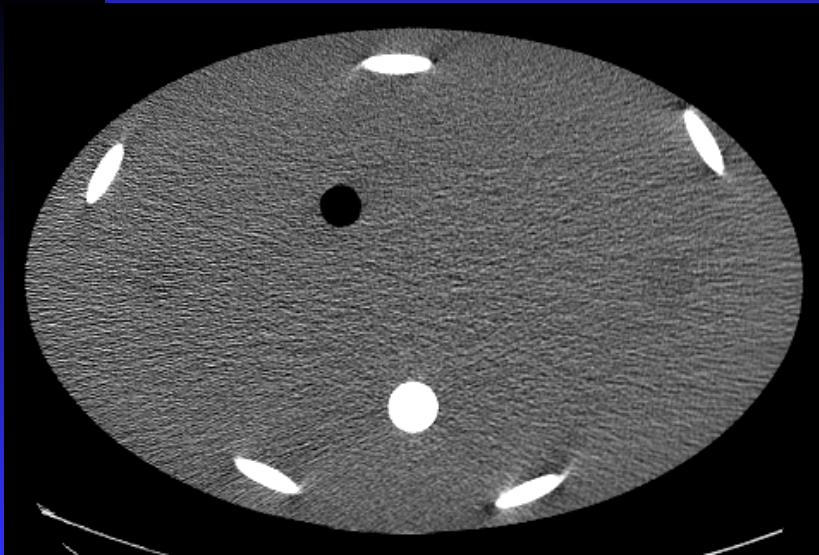
- Slice thickness can be selected by modifying the reconstruction process.
- By low-pass filtering in the z-direction, the slice sensitivity profile can be broadened to any desired shape and thickness.
- From an image artifact point of view, images generated with the thinner slice aperture is better.



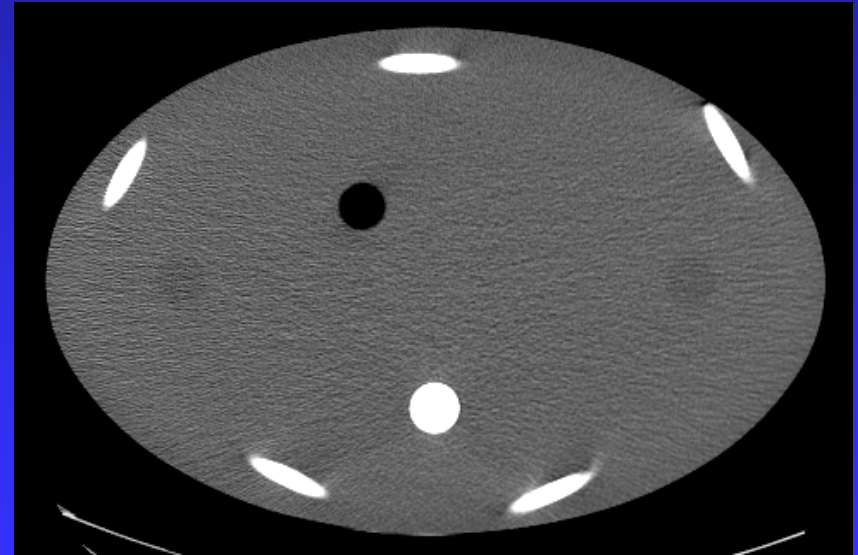
Example

- Z filtering can be applied in either the projection domain or the image domain.
- In general, z-smoothing provides artifact suppression capability.

16x0.625mm detector aperture at 1.75:1 helical pitch



FWHM=0.625mm



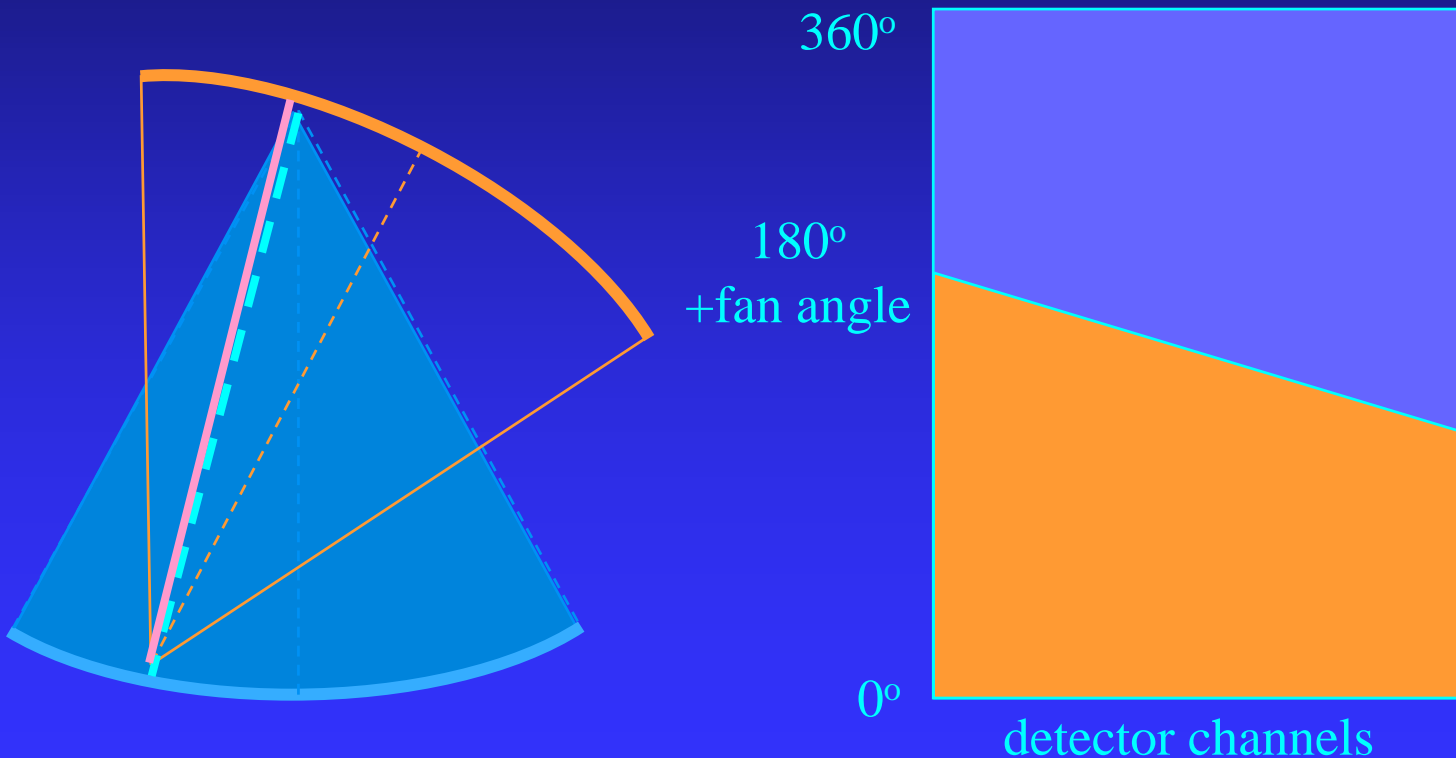
FWHM=2.5mm

Cardiac Scans

- The most challenging problem in cardiac scanning is motion.
- Unlike respiratory motion, cardiac motion cannot be voluntarily controlled.
- For motion suppression, we could either reduce the acquisition time and/or acquire the data during the minimum cardiac motion.
- In cardiac motion, there are relative quiescent period: diastolic phase of the heart motion.

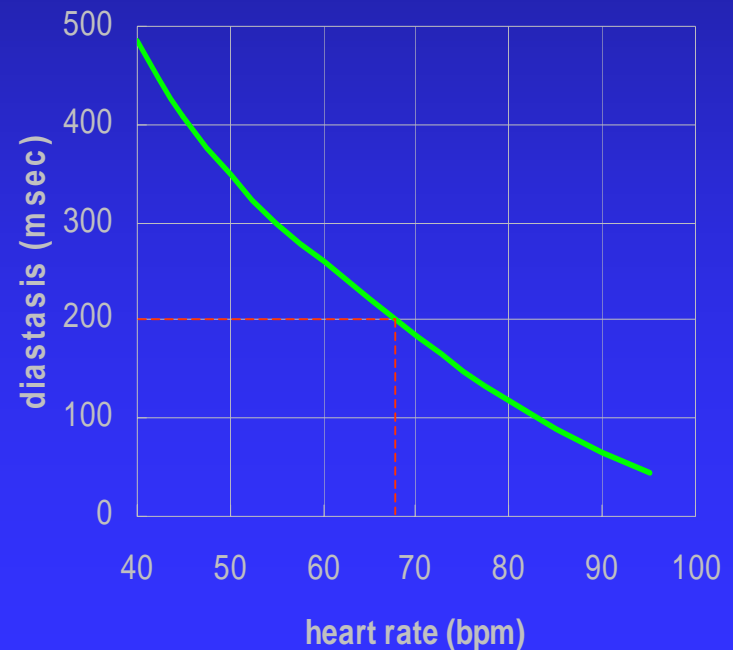
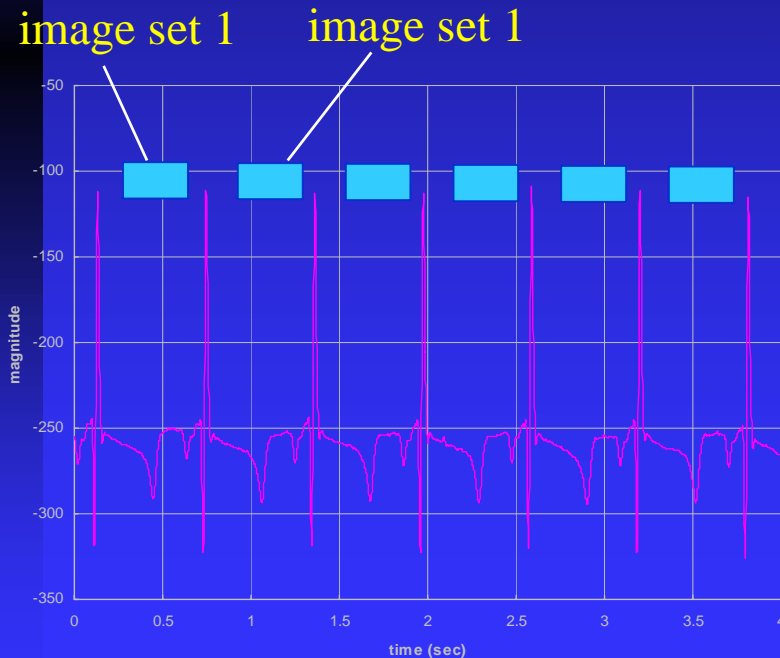
Halfscan

- In fan beam, each ray path is sampled by two conjugate samples.
- We need only $180^\circ + \text{fan angle}$ data for complete reconstruction.



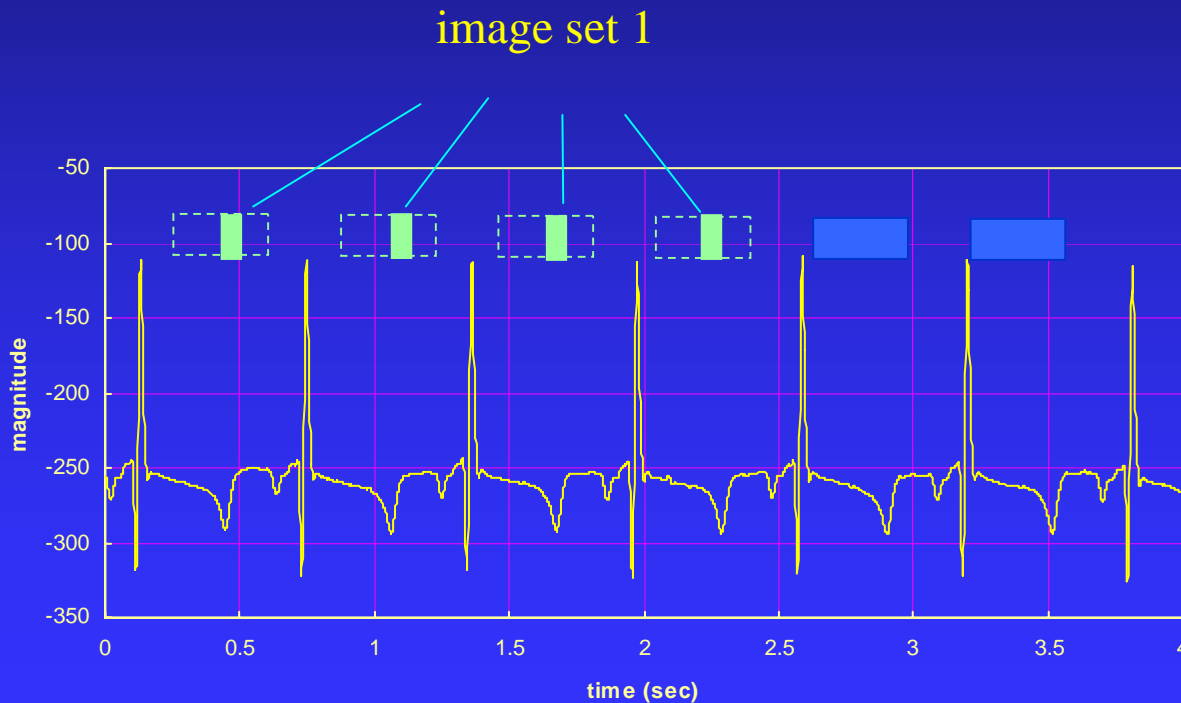
Single-cycle Reconstruction

- Cardiac imaging takes advantage of the quiescent periods in cardiac motion with EKG-gating.
- The duration of quiescent periods change with heart rates.

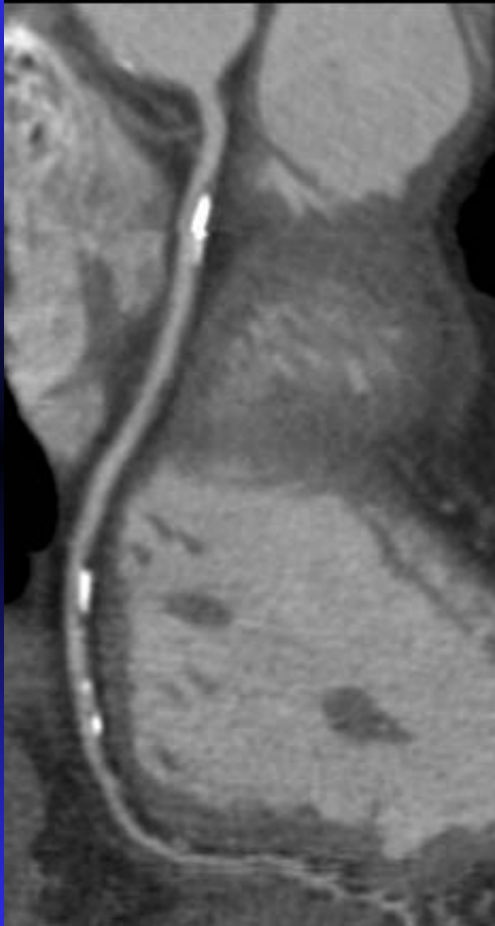


Multi-cycle Cardiac Reconstruction

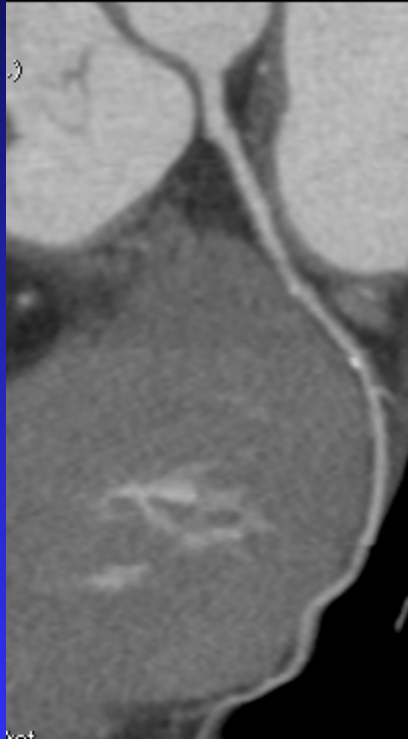
- A complete set of projections is acquired over multiple cardiac cycles to improve temporal resolution.
- The method relies on the regularity of heart motion.



Cardiac Imaging



curved reformation



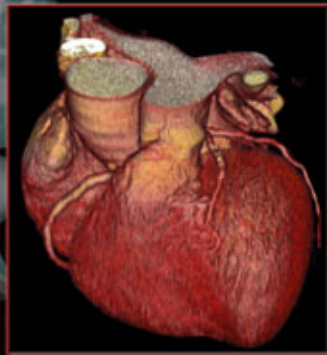
volume rendering

Summary

- Advanced CT Image reconstruction techniques have been continuously developed over the years to keep up with advancements in acquisition hardware and acquisition protocols.
- With the large number of images generated by new CT scanners, advanced visualization tools are required to improve the productivity of radiologists.
- Image reconstruction algorithm not only complement scanner hardware, but also extends the hardware capability.

Computed Tomography:

Principles, Design, Artifacts,
and Recent Advances



Jiang Hsieh

References

- J. Hsieh, *Computed Tomography: principles, design, artifacts, and recent advances*, SPIE Press, 2002.
- J. Hsieh, “CT Image Reconstruction,” in RSNA Categorical Course in *Diagnostic Radiology Physics: CT and US Cross-sectional Imaging 2000*, ed. L. W. Goldman and J. B. Fowlkes, RSNA, 2000; pp. 53-64.
- A. Kak and M. Slaney, *Principles of Computed Tomographic Imaging*, IEEE Press, 1988.

Thank You!